

# Timing Rules for Synaptic Plasticity Matched to Behavioral Function

## Highlights

- Synaptic plasticity rules are not uniform, but tuned to specific circuit function
- Different rules at different cerebellar parallel fiber-to-Purkinje cell synapses
- Synaptic plasticity can precisely compensate for circuit delays of >100 ms
- Provides a mechanism for solving temporal credit assignment problem

## Authors

Aparna Suvrathan, Hannah L. Payne,  
Jennifer L. Raymond

## Correspondence

aparnasu@stanford.edu

## In Brief

Suvrathan et al. expand the known repertoire of synaptic plasticity by showing that the same kind of synapses can exhibit different learning rules and that these rules can precisely compensate for behaviorally relevant circuit delays.

# Timing Rules for Synaptic Plasticity Matched to Behavioral Function

Aparna Suvrathan,<sup>1,2,\*</sup> Hannah L. Payne,<sup>1</sup> and Jennifer L. Raymond<sup>1</sup>

<sup>1</sup>Department of Neurobiology, Stanford University, Stanford, CA 94305, USA

<sup>2</sup>Lead Contact

\*Correspondence: [aparnasu@stanford.edu](mailto:aparnasu@stanford.edu)

<http://dx.doi.org/10.1016/j.neuron.2016.10.022>

## SUMMARY

It is widely assumed that the complexity of neural circuits enables them to implement diverse learning tasks using just a few generic forms of synaptic plasticity. In contrast, we report that synaptic plasticity can itself be precisely tuned to the requirements of a learning task. We found that the rules for induction of long-term and single-trial plasticity at parallel fiber-to-Purkinje cell synapses vary across cerebellar regions. In the flocculus, associative plasticity *in vitro* and *in vivo* is narrowly tuned for an interval of ~120 ms, which compensates for the specific processing delay for error signals to reach the flocculus during oculomotor learning. In the vermis, which supports a range of behavioral functions, plasticity is induced by a range of intervals, with individual cells tuned for different intervals. Thus, plasticity at a single, anatomically defined type of synapse can have properties that vary in a way that is precisely matched to function.

## INTRODUCTION

The algorithm used by a neural circuit to learn is defined by both the circuit-level properties and the rules governing the induction of synaptic plasticity. It has been widely assumed that a few basic synaptic rules, when embedded in the appropriate circuit architecture, can support the full repertoire of learning, in all of its complexity. In contrast, we provide evidence that the synaptic plasticity rules themselves can be highly specialized to match the functional requirements of a learning task.

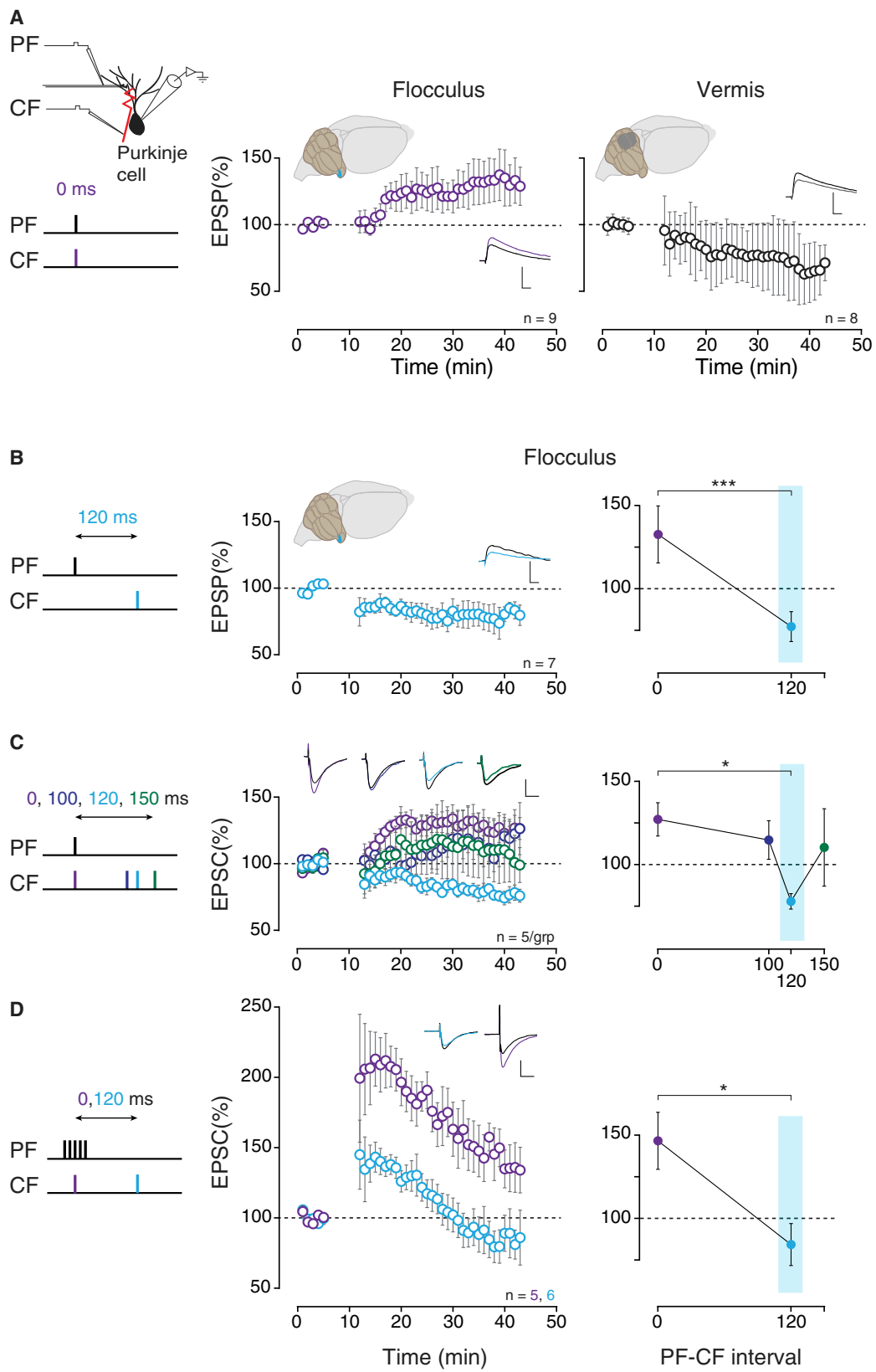
The fundamental requirement of associative learning is to store information about the correlations between events. Throughout the nervous system, synaptic plasticity mechanisms have been described that can capture the correlations between coincident or nearly coincident events (Feldman, 2012). However, behavioral observations indicate that the brain is also able to associate events that are separated in time, with exquisite temporal precision. For example, during feedback-based learning, a delayed error signal must selectively modify synapses active at the specific, earlier time when the neural command leading to an error was generated, a challenge known as the

temporal credit assignment problem (Sutton and Barto, 1981). In throwing a ball, for example, there is a delay of a few hundred milliseconds for the ball to reach the target and for visual feedback about the accuracy of the throw to reach the nervous system. Nevertheless, the timing of the finger movements controlling the release of the ball can be learned with remarkable precision—a difference of just 10 ms can cause the throw to be too high or too low (Hore et al., 1996).

Previously described mechanisms of synaptic plasticity do not seem to have the properties to support such temporally precise learning across delays, without additional, circuit-level timing mechanisms. Known mechanisms of associative synaptic plasticity that have precise timing requirements, such as those underlying spike-timing-dependent plasticity (STDP), are all tuned for neural events occurring within a few tens of milliseconds of each other (Feldman, 2012). Other forms of synaptic plasticity have been described that can associate neural events across longer intervals, but with much less temporal precision (Chen and Thompson, 1995; Debanne et al., 1998; Safo and Regehr, 2008). Therefore, circuit-level mechanisms have been hypothesized to enable known, coincidence-based plasticity mechanisms to support temporally precise learning about events that are separated in time (e.g., Mehta et al., 2002). Here, we show that synaptic plasticity in the cerebellum is itself tuned to meet the dual demands of temporally precise learning in the face of delayed feedback.

During cerebellum-dependent learning, delayed feedback about performance errors is conveyed to the cerebellum by its climbing fiber input. Each spike in a climbing fiber produces a “complex spike” and concomitant calcium influx in its Purkinje cell targets. Repeated pairings of climbing fiber (CF) activation with the activation of parallel fiber (PF) synapses onto the Purkinje cells result in depression of the parallel fiber-to-Purkinje cell (PF-to-PC) synapses (Ito, 2001; Linden, 1994). Thus, error signals carried by the climbing fibers are thought to sculpt away, through associative synaptic depression, PF-to-PC synapses that were active around the time that an error was generated.

The induction of plasticity at PF-to-PC synapses has been characterized as having broad timing requirements, with associative synaptic depression induced when climbing fiber and parallel fiber activation are coincident and also when the climbing fiber activation precedes parallel fiber activation or is delayed by as much as 200 ms (e.g., Chen and Thompson, 1995; Safo and Regehr, 2008). These studies were conducted almost exclusively in the cerebellar vermis, where the climbing fibers encode



(legend on next page)

error signals of multiple modalities and hence a broad range of feedback delays. This heterogeneity makes it difficult to determine the functionally relevant feedback delay for a given climbing fiber *in vitro* and hence to assess the match between the feedback delay and the temporal requirements for the induction of synaptic plasticity. To overcome this challenge, we characterized plasticity at PF-to-PC synapses in a more functionally homogeneous region of the cerebellum, the flocculus. We discovered that the rules governing associative plasticity at PF-to-PC synapses in the flocculus are different than in the vermis and precisely compensate for delays in the error signals in the intact circuit during learning.

## RESULTS

### Heterogeneity in the Rules for Long-Term Plasticity at Cerebellar Parallel Fiber-to-Purkinje Cell Synapses

We compared long-term plasticity at PF-to-PC synapses in the cerebellar flocculus with plasticity at PF-to-PC synapses in the cerebellar vermis in acute slices from adult mice (Figures 1A–1D). We monitored the change in the amplitude of the parallel fiber-elicited excitatory post-synaptic potential (EPSP) in individual Purkinje cells induced by repeated, coincident pairings of a single stimulus to the parallel fibers and to the climbing fibers (300 times at 1 Hz, parallel fiber-climbing fiber [PF-CF] interval of 0 ms; Figure 1A, left). Consistent with previous reports (e.g., Hansel et al., 2006; Ito, 2001), coincident stimulation induced robust long-term depression (LTD) in slices of the cerebellar vermis (Figure 1A, right). In the cerebellar flocculus, however, the results were strikingly different. Instead of inducing LTD, coincident activation of parallel fibers and climbing fibers induced long-term potentiation (LTP) (Figure 1A, center). LTP is the non-associative form of plasticity at the PF-PC synapses, which is induced by parallel fiber activation alone in the vermis (Lev-Ram et al., 2002) and the flocculus (Figure S1A). Hence, the rules governing the induction of associative, climbing fiber-driven plasticity at PF-to-PC synapses are different in the cerebellar flocculus and the cerebellar vermis.

### Long-Term Associative Plasticity in the Flocculus In Vitro: Temporal Requirements Matched to Behavioral Function

Our finding that coincident parallel fiber and climbing fiber stimulation failed to induce LTD in the flocculus was surprising, given

the multiple lines of evidence for a role of climbing fiber-triggered LTD in flocculus-dependent learning (e.g., Boyden et al., 2006; Hansel et al., 2006; Ito, 2001; Kimpo et al., 2014; Medina and Lisberger, 2008). However, *in vivo*, the activation of climbing fibers by performance errors would be delayed relative to the parallel fiber activity that caused the error, rather than coincident. Therefore, we tested whether LTD could be induced in the flocculus when climbing fiber activation was delayed, as would occur *in vivo* during learning. The function of the flocculus is to regulate the smooth eye movements that stabilize images on the retina (Ito, 2001; du Lac et al., 1995); therefore, retinal image motion represents a performance error. Visual feedback about such errors is encoded by climbing fibers in the flocculus at a delay of about 120 ms (Figure S1B; Maekawa and Simpson, 1973; Raymond and Lisberger, 1998; Stone and Lisberger, 1986). *In vivo* experiments have suggested that there must be some form of compensation for this delay in order to support the adaptive recalibration of eye movements observed across a range of visual and vestibular stimulus frequencies (Ramachandran and Lisberger, 2005; Raymond and Lisberger, 1998, 2000). More specifically, it can be estimated that it would be optimal for climbing fiber activity to induce plasticity at synapses active ~120 ms earlier (Figure S1B).

Consistent with this circuit-level constraint on feedback-based learning, robust LTD was induced in floccular slices when parallel fibers were activated 120 ms before the climbing fibers (Figure 1B). Thus, plasticity at PF-to-PC synapses in the flocculus not only differs from plasticity at PF-to-PC synapses in the vermis, but also compensates for the relevant error signal delay.

These results, from experiments in which PF-to-PC synaptic strength was measured in current clamp (Figures 1A and 1B; Figures S1Ci and S1D), were replicated in additional experiments that measured synaptic strength in voltage clamp (Figure 1C; Figures S1Cii). In addition, the tuning of LTD in the flocculus to the PF-CF interval was tested by comparing four different intervals (Figure 1C): 0 ms (coincident, purple), 100 ms (dark blue), 120 ms (light blue), and 150 ms (green). Although a climbing fiber delay of 120 ms relative to the parallel fibers induced robust LTD, neither a climbing fiber delay of 100 ms nor a delay of 150 ms was effective at inducing LTD. Thus, the tuning of LTD for the PF-CF interval was remarkably selective, with a narrow window for associative plasticity of, at most, a few tens of milliseconds.

**Figure 1. Induction Rules for Cerebellar LTD Are Different in the Flocculus Than the Vermis and Are Tuned to Climbing Fiber Delay**

Long-term plasticity at parallel fiber-to-Purkinje cell (PF-to-PC) synapses was induced with repeated pairings of parallel fiber (PF) and climbing fiber (CF) activation (300 times at 1 Hz). The PF-CF pairing interval was varied, as indicated by schematics on the left of each panel and corresponding colors.

- (A) Coincident PF and CF stimulation (0 ms PF-CF interval, purple) induced long-term potentiation (LTP) of PF-to-PC synapses in the cerebellar flocculus (center) but long-term depression (LTD) of PF-to-PC synapses in lobules V/VI of the cerebellar vermis (right).
- (B) Left, center: in the flocculus, LTD was induced when CF stimulation was delayed by 120 ms relative to PF stimulation (light blue). Right: average EPSP amplitude in the last 10 min of current clamp recordings in the flocculus when the PF-CF pairing interval was 0 ms versus 120 ms. \*\*\*p < 0.001, Mann-Whitney test.
- (C) Long-term plasticity at PF-to-PC synapses in the flocculus measured in voltage clamp for different PF-CF pairing intervals: 0 ms (purple) and 100 ms (dark blue) induced LTP, 120 ms (light blue) induced LTD, and 150 ms (green) induced no significant plasticity. \*p < 0.05, Kruskal-Wallis analysis of variance on ranks followed by pairwise Dunn's test.
- (D) Long-term plasticity at PF-to-PC synapses in the flocculus induced by pairing trains of PF stimulation (5 at 100 Hz) with CF stimulation (300 times at 1 Hz). A PF-CF interval of 0 ms (purple) induced LTP, whereas 120 ms (light blue) induced LTD. \*p < 0.05, Mann-Whitney test. n = number of cells. Insets show EPSPs or EPSCs from an example cell just prior to plasticity induction (black) and 30 min later (color); scale bars, 5 mV or 200 pA, 20 ms.

All panels are mean ± SEM. See also Figures S1A–S1F.

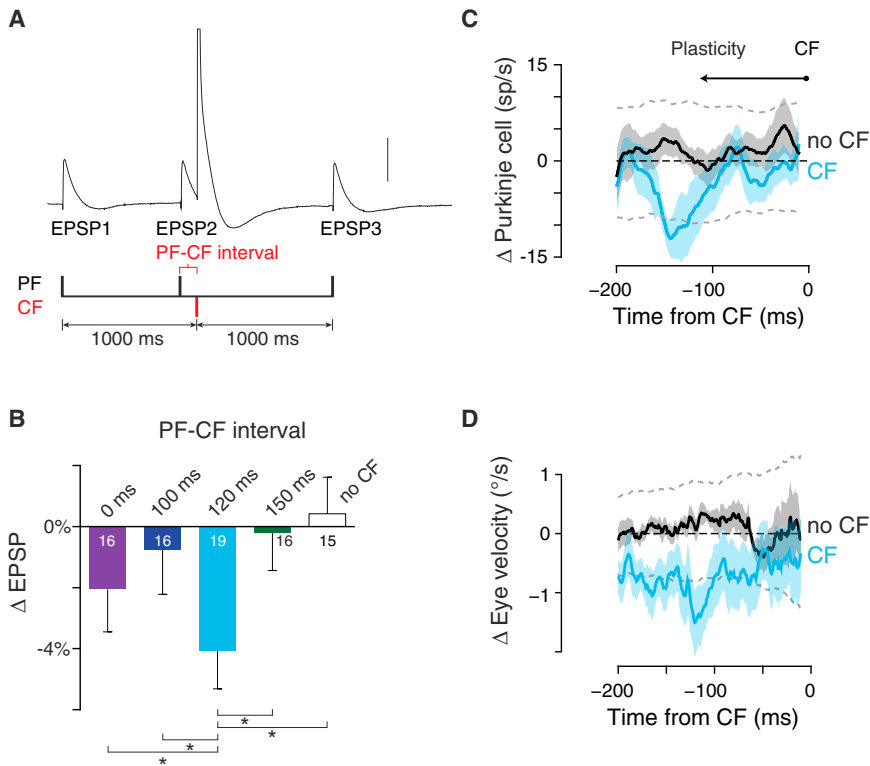


**Figure 2. Similar Temporal Tuning of Single-Trial Plasticity in the Flocculus In Vitro and In Vivo**

(A) The synaptic response in the Purkinje cell to parallel fiber stimulation was compared before (EPSP1) and after (EPSP3) a single pairing of PF and climbing fiber stimulation. Stimulus artifact and spike elicited by CF truncated. Scale bar, 10 mV.

(B) Change in the amplitude of EPSP3 relative to EPSP1 ( $\Delta$ EPSP, mean  $\pm$  SEM) for different PF-CF pairing intervals and for controls with no CF stimulation (no CF). Single-trial depression of parallel fiber-to-Purkinje cell synapses in the flocculus was selectively induced by a 120 ms PF-CF pairing interval. Number of cells is indicated in each bar. \* $p < 0.05$  repeated-measures ANOVA on ranks, followed by pairwise post hoc Student-Newman-Keuls comparison.

(C and D) Trial-to-trial changes in Purkinje cell firing (C) and eye movement responses (D) in vivo during oculomotor learning were precisely timed to compensate for delays in the error signals carried by climbing fibers. Pairs of consecutive trials were analyzed by subtracting the Purkinje cell's simple spike firing rate or the eye movement response during the second trial of the pair from that on the first trial, averaged across trials of a given type, and then across cells. If there was a spike in the climbing fiber on the first trial of the pair (CF, blue traces), there was a decrease in Purkinje cell firing and a change in the eye movement response on the next trial, at a time

corresponding to  $\sim$ 120 ms before the time of the CF spike on the first trial. If there was no spike in the climbing fiber (no CF, black traces), there was no trial-to-trial change. Dotted lines indicate 95% confidence intervals determined by bootstrap.

All panels are mean  $\pm$  SEM. See also *Supplemental Experimental Procedures* and Figures S2A–S2G.

To test the generality of this timing requirement, we compared the effectiveness of coincident versus delayed climbing fiber activation when it was paired with a brief, high-frequency train of parallel fiber stimulation (5 PF stimuli at 100 Hz, paired with the CF, 300 times at 1 Hz; Figure 1D). When PF trains were paired with coincident climbing fiber stimulation (PF-CF interval, 0 ms), PF-to-PC synapses in the flocculus underwent a robust LTP (Figure 1D, purple) rather than the LTD that was previously reported in the vermis for similar pairing protocols (Safo and Regehr, 2008; Wang et al., 2000). However, if parallel fiber trains were instead paired with climbing fiber stimulation delayed by 120 ms, there was a transient potentiation of PF-to-PC synapses in the flocculus, followed by LTD (Figure 1D, light blue). Notably, the synapses that underwent pairing at a PF-CF interval of 120 ms were less potentiated/more depressed than those that underwent coincident PF-CF pairing throughout the entire post-pairing period (Figure 1D; Figures S1Cii). LTD was pathway specific (Figure S1E), as previously described for LTD in the vermis (Ekerot and Kano, 1985; see also Linden, 1994). Moreover, the LTD induced in the flocculus using both single parallel fiber pulses and trains appeared to be expressed post-synaptically, as previously described for cerebellar LTD (e.g., Finch and Augustine, 1998), since there was no change in the paired-pulse ratio (Figures S1D).

### Single-Trial, Short-Term Associative Plasticity in the Flocculus In Vitro: Temporal Requirements Matched to Behavioral Function

It was recently reported that a single spike in a climbing fiber in vivo can induce plasticity (Kimpo et al., 2014; Medina and Lisberger, 2008; Yang and Lisberger, 2010). We tested whether there was short-term plasticity at the PF-to-PC synapses in response to a single pairing of parallel fiber and climbing fiber activation (see also Brenowitz and Regehr, 2005), which could support the single-trial plasticity observed in vivo during motor learning.

In slices from the mouse cerebellar flocculus, the change in the strength of the PF-to-PC EPSP was measured from test stimuli delivered 1 s before and 1 s after a single pairing of parallel fiber and climbing fiber activation (Figure 2A; Figure S2A). These single trials were delivered at an inter-trial interval of 7 s (see *Supplemental Experimental Procedures*), and the change in the PF-to-PC EPSP measured on single trials was averaged over  $\sim$ 25 trials for each pairing condition. As a control, the PF-CF pairing was replaced by a PF stimulus alone (Figure 2B; Figures S2A–S2C, no CF) or a climbing fiber stimulus alone (Figure S2D, no PF), in which case there was no change, on average, in the PF-to-PC EPSP. However, a single pairing of climbing fiber activation 120 ms after parallel fiber activation induced a significant depression of the PF-to-PC EPSP (Figure 2B; Figures S2Aii,

S2Bii–S2Biv, and S2D, light blue). This single-trial synaptic plasticity was not only rapidly induced, but also recovered rapidly, returning to baseline prior to the next trial (Figure S3B). The rapid recovery allowed multiple PF-CF intervals to be tested on the same cell. On average, PF-CF intervals of 0, 100, and 150 ms induced significantly less depression than an interval of 120 ms (Figure 2B; see Figures S2E and S2F for additional controls). Hence, the temporal specificity for the PF-CF interval in the flocculus was similar for the induction of LTD by multiple PF-CF pairings and for the induction of short-term depression by a single PF-CF pairing.

### During Associative Learning In Vivo, Plasticity of Floccular Purkinje Cells Exhibits Precise Compensation for Feedback Delays

The single-trial depression observed at PF-to-PC synapses in response to a single PF-CF pairing *in vitro* provides a candidate mechanism for trial-to-trial changes in Purkinje cell firing observed *in vivo*. During oculomotor learning, a spike in a climbing fiber on one trial is associated with a suppression of firing in its Purkinje cell target on the next trial (Kimpo et al., 2014; Medina and Lisberger, 2008; Yang and Lisberger, 2010, 2014). The temporal precision of this single-trial plasticity reported *in vivo* had appeared to be significantly less than what we found at the PF-to-PC synapses *in vitro* (hundreds of milliseconds versus tens of milliseconds). However, previous studies of trial-to-trial changes *in vivo* had aligned on the trial start time, whereas the *in vitro* results (Figures 1 and 2B) suggested that plasticity might occur at synapses active in a specific time window preceding the climbing fiber spike. Therefore, we aligned changes in Purkinje cell firing during vestibulo-ocular reflex (VOR) learning in rhesus monkeys (Kimpo et al., 2014) to the time of the climbing fiber spike in the preceding trial (Figure 2C; Figure S2G; Supplemental Experimental Procedures). If there was no spike in a given climbing fiber on one trial, then there was no detectable change in the firing rate of its Purkinje cell target on the next trial (Figure 2C, no CF, black trace). However, if there was a spike in the climbing fiber on one trial, then there was a reduction in the Purkinje cell firing rate on the next trial (Figure 2C, CF, blue trace). Remarkably, the reduction in firing occurred at a time within the trial corresponding to ~120 ms prior to the time of the climbing fiber spike on the previous trial and then rapidly returned to baseline before the time of the climbing fiber spike. This suggests that, *in vivo*, a climbing fiber spike triggers plasticity at synapses active ~120 ms earlier and not at synapses active coincidentally. Accompanying the changes in Purkinje cell firing were adaptive changes in eye velocity that were also precisely timed (Figure 2D) and slightly delayed relative to the altered Purkinje cell responses, suggesting a causal relationship.

Thus, *in vivo*, single-trial, climbing fiber-triggered plasticity in the flocculus of rhesus monkeys has temporal properties similar to the single-trial depression of the PF-to-PC synapses in floccular slices from mice. Both have the temporal precision to precisely compensate, to within a few tens of milliseconds, for the ~120 ms delay in the error signals carried by climbing fibers during eye movements in both species (Figure S1B). In addition, it suggests that there is sufficient temporal precision in the patterns of activation of the parallel fibers to provide a substrate

for the temporally precise plasticity (Fujita, 1982; Medina and Mauk, 2000; Yamazaki and Tanaka, 2009; but see Johansson et al., 2014).

### Heterogeneity in the Rules for Single-Trial, Short-Term Plasticity at Cerebellar Parallel Fiber-to-Purkinje Cell Synapses

As observed for LTD, we found that the induction of single-trial depression at the PF-to-PC synapses is governed by different rules in the cerebellar vermis than in the flocculus. However, by leveraging the ability to test an individual cell with multiple PF-CF intervals, we uncovered temporal precision of the single-trial plasticity in the vermis comparable to that in the flocculus.

In contrast to the flocculus, a broad range of PF-CF intervals was effective at inducing single-trial synaptic depression at PF-to-PC synapses in the vermis. A single, coincident PF-CF pairing (Figure 3A, 0 ms), as well as climbing fiber stimulation delayed by intervals as long as 150 ms relative to parallel fiber stimulation, induced significant depression at PF-to-PC synapses, as measured in the population average (Figure 3A; Figure S3A). This broad temporal window for the induction of single-trial depression at PF-to-PC synapses in the vermis is similar to what has been described previously for long-term depression at the same synapses (e.g., Safo and Regehr, 2008). However, broad tuning at the population level masked precise temporal requirements for the single-trial plasticity in individual cells.

The cells recorded in the vermis (Figure 3A) were sorted according to their preferred PF-CF interval, i.e., the one that produced the biggest single-trial depression (Figure 3B). Notably, cells that preferred a given interval underwent no significant depression at any of the other PF-CF intervals (Figure 3B, repeated-measures ANOVA).

The tuning of plasticity to the PF-CF interval was quantified with a selectivity index (SI) (Figure 3F):

$$SI = \frac{D_{Pref} - D_{NonPref}}{D_{Pref}}$$

where  $D_{Pref}$  = depression at the preferred interval, and  $D_{NonPref}$  = average depression at non-preferred intervals.

At the population level, the selectivity index was close to zero in the vermis, indicating almost no selectivity, whereas the selectivity index was 0.6 for the flocculus, indicating considerable selectivity (Figure 3F, left). However, when the selectivity index was calculated for individual cells, the mean was greater than 0.6 in both regions and not significantly different between the two regions (Figure 3F, right). Thus, individual cells in both regions were tuned for the PF-CF interval. The key difference between regions is that, in the flocculus, the majority of cells prefer the same, behaviorally relevant climbing fiber delay of 120 ms, whereas in lobules V/VI of the vermis, different cells prefer different intervals.

We leveraged this variability across cells to look for electrophysiological correlates of the preferred interval for inducing synaptic depression. Cells that preferred different PF-CF intervals had no detectable difference in the baseline EPSP amplitude or spatial localization within lobules V and VI (Figures S3Ci and S3Cii). However, one electrophysiological signature

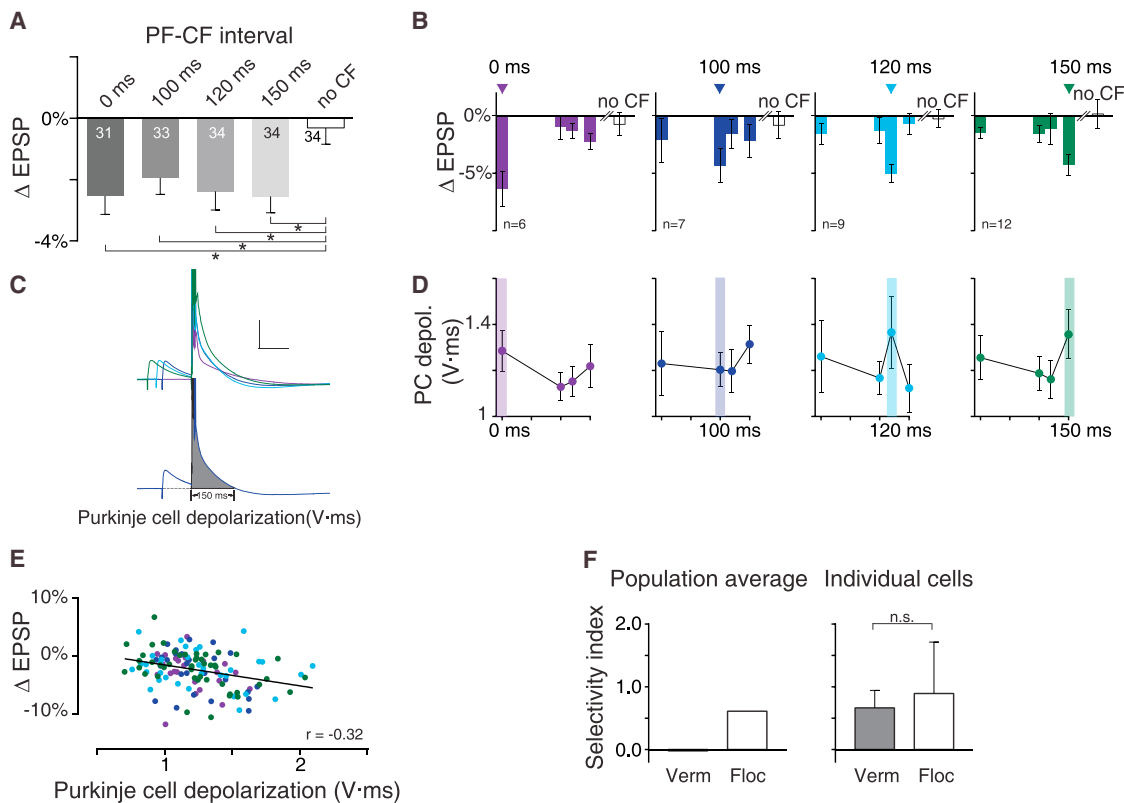


**Figure 3. In the Vermis, Single-Trial Depression at the Parallel Fiber-to-Purkinje Cell Synapses Is Induced by a Range of Parallel Fiber-Climbing Fiber Pairing Intervals**

(A) Single-trial synaptic plasticity in the vermis, measured as in Figures 2A and 2B. \* $p < 0.05$ , repeated-measures ANOVA, followed by pairwise post hoc Student-Newman-Keuls comparison.

(B) Cells in (A) were sorted according to the PF-CF interval that induced the maximum depression, the “preferred interval” (arrowheads). There was no significant depression at any PF-CF interval, except the preferred interval, for any subgroup of cells (repeated-measures ANOVA),  $n$  = number of cells.

(C) Top: traces from a single cell showing different amount of Purkinje cell depolarization for different PF-CF pairing intervals (indicated by color). This cell showed maximal depression for a PF-CF interval of 150 ms. Spike truncated. Bottom: gray shading indicates the area measured to quantify the Purkinje cell depolarization.

(D) Purkinje cell depolarization for each PF-CF interval in each sub-group of cells; cells sorted as in (B) according to the interval inducing the greatest depression (highlighted).

(E) Synaptic depression ( $\Delta$ EPSP) in each cell for each PF-CF interval was correlated with the amount of Purkinje cell depolarization during PF-CF pairing. See also Figure S3D.

(F) A selectivity index (SI), quantifying the tuning of single-trial depression for the PF-CF pairing interval, was calculated for the population averages shown in Figures 2B and 3A and for the individual cells contributing to those averages,  $SI = (\text{Depression}_{\text{Preferred}} - \text{Avg. Depression}_{\text{Non-preferred}})/\text{Depression}_{\text{Preferred}}$  (see *Supplemental Experimental Procedures*). The population average (left) reveals no selectivity in the vermis (selectivity index very close to zero) in contrast to the flocculus; however, the selectivity index for individual cells in the vermis was not significantly different from that in the flocculus (right, Mann-Whitney test).

All panels are mean  $\pm$  SEM. See also Figures S3A–S3D.

was identified that predicted the amount of depression. In individual cells, the extent to which the Purkinje cell depolarized during the complex spike elicited by CF stimulation varied with the PF-CF interval (Figure 3D), and the PF-CF interval that induced the greatest depolarization of the Purkinje cell tended to be the one that induced the greatest single-trial depression (Figures 3D and 3E; Figure S3D). Previously, the size of the complex spike has been correlated with the amplitude of the calcium transient and the induction of plasticity (e.g., Kitamura and Häusser, 2011; Mathy et al., 2009; Wang et al., 2000; Yang and Lisberger, 2014). Our results extend these previous observations by

showing that the size of the complex spike, as measured by the amount of depolarization, varies with the PF-CF interval.

## DISCUSSION

Our findings prompt a rethinking of the common assumption that the properties of synaptic plasticity are uniform across an anatomically defined type of synapse. Given the “crystalline” cytoarchitecture of the cerebellum, it has been widely assumed that the properties of synaptic plasticity that have been described in the vermis apply throughout the cerebellum.

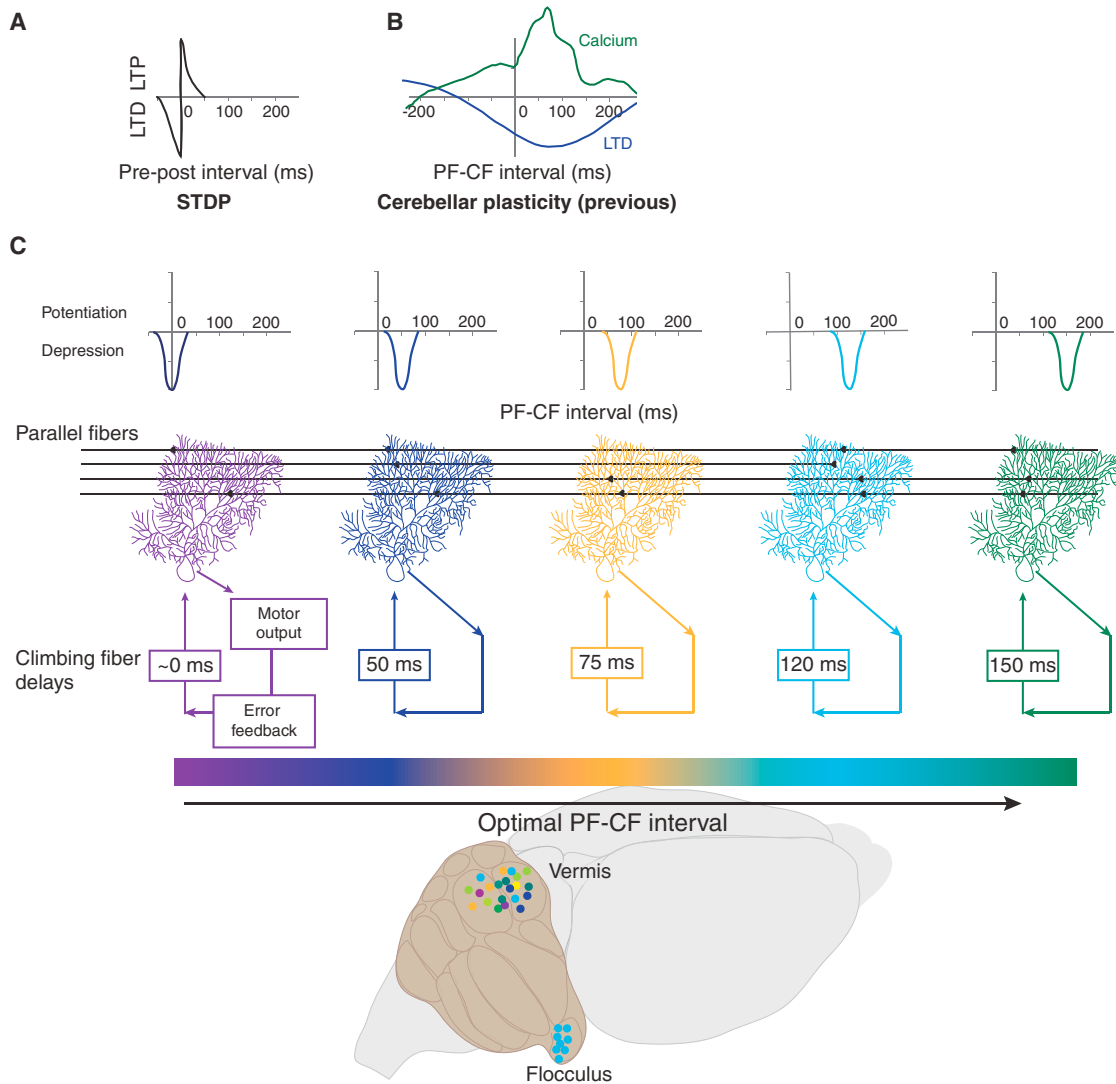


**Figure 4. Synaptic Mechanisms for Learning a Range of Behaviorally Relevant Temporal Correlations**

(A) Schematic based on previous findings of spike-timing-dependent plasticity (STDP) showing precise induction of plasticity for short inter-event intervals centered around coincident pre- and post-synaptic inputs (Bi and Poo, 1998; Markram et al., 1997).

(B) Schematic based on previous findings in the cerebellum illustrating calcium increases (green; Wang et al., 2000) and synaptic plasticity (LTD, blue; Safo and Regehr, 2008) induced by a broad range of PF-CF intervals extending out to hundreds of milliseconds.

(C) Top: schematic of plasticity in the cerebellum, based on current data, showing each cell narrowly tuned to a single PF-CF interval, and different cells tuned for different intervals, together spanning a range of >100 ms. Schematics in (A)–(C) are on the same timescale. Bottom: in each region of the cerebellum, the population of cells (colored circles) may tile the space of functionally relevant intervals for the behaviors supported by that region. In regions like the flocculus, with a uniform error-signal delay, cells (light blue circles) are more uniformly tuned to a single, behaviorally relevant interval.

See also Figures S4A and S4B.

However, there are known differences in gene expression, Purkinje cell firing rates, and behavioral functions of different cerebellar regions (Cerminara et al., 2015) and a report that some regions exhibit less PF-to-PC LTD than others (Wadiche and Jahr, 2005). Our results suggest that all regions of the cerebellum may undergo PF-to-PC LTD, but the rules for the induction of this plasticity may be different. We found different rules for depression of the PF-to-PC synapses in different functional regions of the cerebellum (flocculus versus vermis; Figures 1A, 2B, and

3A) and even different cells within a small region (lobules V/VI of vermis; Figure 3B).

In the vermis, associative synaptic depression can be induced by a wide range of delays between parallel fiber and climbing fiber activation. This wide range of effective delays may reflect the wide range of delays in the error signals carried by the different climbing fiber inputs to the cerebellar vermis, which supports behavioral functions ranging from postural to cognitive (Menghini et al., 2013; Stoodley et al., 2012). For example, climbing

fiber inputs to lobules V/VI of the vermis, where the *in vitro* studies of single-trial synaptic plasticity shown in Figures 3A–F were conducted, carry signals ranging from spinal afferent signals with latencies as short as 10–30 ms (Berthoz and Llinás, 1974) to cognitive signals with presumably much longer latencies (Menghini et al., 2013).

In the flocculus, tuning to the PF-CF interval was much more uniform so that it was evident in the population average as well as in individual cells. Depression was reliably induced by a climbing fiber delay of 120 ms and not by coincident climbing fiber activation or by climbing fiber delays just a few tens of milliseconds greater or less than 120 ms. Tuning for the same 120 ms delay was observed in the flocculus over a wide range of conditions: using trains of parallel fiber stimuli as well as single parallel fiber stimuli during LTD induction, in separate experiments measuring LTD in current clamp and voltage clamp, for short-term, as well as long-term, plasticity, and *in vivo* as well as *in vitro*. This tuning for the PF-CF interval provides a synaptic mechanism for the circuit to solve a major component of the temporal credit assignment problem by precisely compensating, to within a few tens of milliseconds, for delays in the feedback about errors carried by climbing fibers *in vivo* (Figures S4A and S4B).

The synaptic plasticity that we describe expands the known repertoire of cellular mechanisms available to neural circuits for making associations between non-coincident events over a wide range of time intervals (Figures 4A and 4B). Other known forms of plasticity with precise timing requirements for induction, such as STDP, are tuned for inter-event intervals close to coincident (Figure 4A). Such forms of plasticity provide a mechanism for distinguishing the *order* in which neurons fire and hence causality. In contrast, the narrow tuning of plasticity at the PF-to-PC synapses to much longer intervals provides a mechanism, not just for distinguishing the order, but also for encoding the precise *timing* between neural events.

The discovery of precise tuning of synaptic plasticity to a behaviorally relevant inter-event interval was facilitated by the uniform and well-characterized function of the cerebellar flocculus. However, each region of the cerebellum may contain an array of synaptic detectors that are tuned either through evolution or through metaplasticity so that the population tiles the range of parallel fiber-climbing fiber intervals relevant to the behaviors supported by that region (Figure 4C). It is intriguing to speculate that such tuning may be a more widespread property of synapses throughout the brain. In the particular case of Purkinje cells, all synapses onto a given cell may be tuned to the same interval, determined by the characteristic delay of the error signals carried by the single climbing fiber input to that cell. However, for other types of neurons, even different synapses onto the same cell might obey different plasticity rules if the synapses are part of different circuits. Thus, a diversity of synaptic learning rules may work in conjunction with circuit-level mechanisms to learn the temporal correlations between events in the natural world.

## EXPERIMENTAL PROCEDURES

See Supplemental Experimental Procedures.

## SUPPLEMENTAL INFORMATION

Supplemental Information includes Supplemental Experimental Procedures and four figures and can be found with this article online at <http://dx.doi.org/10.1016/j.neuron.2016.10.022>.

## AUTHOR CONTRIBUTIONS

A.S. and J.L.R. planned the experiments, A.S. performed and analyzed the *in vitro* experiments, H.L.P. analyzed the *in vivo* data, and A.S. and J.L.R. wrote the paper.

## ACKNOWLEDGMENTS

We thank J. Burnett for his support through the BioX NeuroVentures Fund; W. Newsome, S. Lisberger, L. Giocomo, L. Frank, B. Nguyen-Vu, T. Manninen, A. Shakhawat, J. Bant, and A. Hayer for helpful input; M. Fu for technical help; and E. Knudsen and L. Giocomo for use of equipment. This work was supported by NIH RO1 NS072406 and RO1 DC004154. A.S. was supported by a Katherine McCormick postdoctoral fellowship. H.L.P. was supported by NSF graduate research fellowship DGE-114747 and NSF IGERT Traineeship 0801700.

Received: September 9, 2015

Revised: July 15, 2016

Accepted: October 7, 2016

Published: November 10, 2016; corrected online February 8, 2018

## REFERENCES

- Berthoz, A., and Llinás, I. (1974). Afferent neck projection to the cat cerebellar cortex. *Exp. Brain Res.* 20, 385–401.
- Bi, G.Q., and Poo, M.M. (1998). Synaptic modifications in cultured hippocampal neurons: dependence on spike timing, synaptic strength, and postsynaptic cell type. *J. Neurosci.* 18, 10464–10472.
- Boyden, E.S., Katoh, A., Pyle, J.L., Chatila, T.A., Tsien, R.W., and Raymond, J.L. (2006). Selective engagement of plasticity mechanisms for motor memory storage. *Neuron* 51, 823–834.
- Brenowitz, S.D., and Regehr, W.G. (2005). Associative short-term synaptic plasticity mediated by endocannabinoids. *Neuron* 45, 419–431.
- Cerminara, N.L., Lang, E.J., Sillitoe, R.V., and Apps, R. (2015). Redefining the cerebellar cortex as an assembly of non-uniform Purkinje cell microcircuits. *Nat. Rev. Neurosci.* 16, 79–93.
- Chen, C., and Thompson, R.F. (1995). Temporal specificity of long-term depression in parallel fiber-Purkinje synapses in rat cerebellar slice. *Learn. Mem.* 2, 185–198.
- Debanne, D., Gähwiler, B.H., and Thompson, S.M. (1998). Long-term synaptic plasticity between pairs of individual CA3 pyramidal cells in rat hippocampal slice cultures. *J. Physiol.* 507, 237–247.
- du Lac, S., Raymond, J.L., Sejnowski, T.J., and Lisberger, S.G. (1995). Learning and memory in the vestibulo-ocular reflex. *Annu. Rev. Neurosci.* 18, 409–441.
- Ekerot, C.F., and Kano, M. (1985). Long-term depression of parallel fibre synapses following stimulation of climbing fibres. *Brain Res.* 342, 357–360.
- Feldman, D.E. (2012). The spike-timing dependence of plasticity. *Neuron* 75, 556–571.
- Finch, E.A., and Augustine, G.J. (1998). Local calcium signalling by inositol-1,4,5-trisphosphate in Purkinje cell dendrites. *Nature* 396, 753–756.
- Fujita, M. (1982). Adaptive filter model of the cerebellum. *Biol. Cybern.* 45, 195–206.
- Hansel, C., de Jeu, M., Belmeguenai, A., Houtman, S.H., Buitendijk, G.H.S., Andreev, D., De Zeeuw, C.I., and Elgersma, Y. (2006). alphaCaMKII is essential for cerebellar LTD and motor learning. *Neuron* 51, 835–843.

- Hore, J., Watts, S., and Tweed, D. (1996). Errors in the control of joint rotations associated with inaccuracies in overarm throws. *J. Neurophysiol.* 75, 1013–1025.
- Ito, M. (2001). Cerebellar long-term depression: characterization, signal transduction, and functional roles. *Physiol. Rev.* 81, 1143–1195.
- Johansson, F., Jireheden, D.A., Rasmussen, A., Zucca, R., and Hesslow, G. (2014). Memory trace and timing mechanism localized to cerebellar Purkinje cells. *Proc. Natl. Acad. Sci. USA* 111, 14930–14934.
- Kimpo, R.R., Rinaldi, J.M., Kim, C.K., Payne, H.L., and Raymond, J.L. (2014). Gating of neural error signals during motor learning. *eLife* 3, e02076.
- Kitamura, K., and Häusser, M. (2011). Dendritic calcium signaling triggered by spontaneous and sensory-evoked climbing fiber input to cerebellar Purkinje cells in vivo. *J. Neurosci.* 31, 10847–10858.
- Lev-Ram, V., Wong, S.T., Storm, D.R., and Tsien, R.Y. (2002). A new form of cerebellar long-term potentiation is postsynaptic and depends on nitric oxide but not cAMP. *Proc. Natl. Acad. Sci. USA* 99, 8389–8393.
- Linden, D.J. (1994). Long-term synaptic depression in the mammalian brain. *Neuron* 12, 457–472.
- Maekawa, K., and Simpson, J.I. (1973). Climbing fiber responses evoked in vestibulocerebellum of rabbit from visual system. *J. Neurophysiol.* 36, 649–666.
- Markram, H., Lubke, J., Frotscher, M., and Sakmann, B. (1997). Regulation of synaptic efficacy by coincidence of postsynaptic APs and EPSPs. *Science* 275, 213–215.
- Mathy, A., Ho, S.S.N., Davie, J.T., Duguid, I.C., Clark, B.A., and Häusser, M. (2009). Encoding of oscillations by axonal bursts in inferior olive neurons. *Neuron* 62, 388–399.
- Medina, J.F., and Lisberger, S.G. (2008). Links from complex spikes to local plasticity and motor learning in the cerebellum of awake-behaving monkeys. *Nat. Neurosci.* 11, 1185–1192.
- Medina, J.F., and Mauk, M.D. (2000). Computer simulation of cerebellar information processing. *Nat. Neurosci.* 3 (Suppl), 1205–1211.
- Mehta, M.R., Lee, A.K., and Wilson, M.A. (2002). Role of experience and oscillations in transforming a rate code into a temporal code. *Nature* 417, 741–746.
- Menghini, D., Di Paola, M., Murri, R., Costanzo, F., Caltagirone, C., Vicari, S., and Petrosini, L. (2013). Cerebellar vermis abnormalities and cognitive functions in individuals with Williams syndrome. *Res. Dev. Disabil.* 34, 2118–2126.
- Ramachandran, R., and Lisberger, S.G. (2005). Normal performance and expression of learning in the vestibulo-ocular reflex (VOR) at high frequencies. *J. Neurophysiol.* 93, 2028–2038.
- Raymond, J.L., and Lisberger, S.G. (1998). Neural learning rules for the vestibulo-ocular reflex. *J. Neurosci.* 18, 9112–9129.
- Raymond, J.L., and Lisberger, S.G. (2000). Hypotheses about the neural trigger for plasticity in the circuit for the vestibulo-ocular reflex. *Prog. Brain Res.* 124, 235–246.
- Safo, P., and Regehr, W.G. (2008). Timing dependence of the induction of cerebellar LTD. *Neuropharmacology* 54, 213–218.
- Stone, L.S., and Lisberger, S.G. (1986). Detection of tracking errors by visual climbing fiber inputs to monkey cerebellar flocculus during pursuit eye movements. *Neurosci. Lett.* 72, 163–168.
- Stoodley, C.J., Valera, E.M., and Schmahmann, J.D. (2012). Functional topography of the cerebellum for motor and cognitive tasks: an fMRI study. *Neuroimage* 59, 1560–1570.
- Sutton, R.S., and Barto, A.G. (1981). Toward a modern theory of adaptive networks: expectation and prediction. *Psychol. Rev.* 88, 135–170.
- Wadiche, J.I., and Jahr, C.E. (2005). Patterned expression of Purkinje cell glutamate transporters controls synaptic plasticity. *Nat. Neurosci.* 8, 1329–1334.
- Wang, S.S., Denk, W., and Häusser, M. (2000). Coincidence detection in single dendritic spines mediated by calcium release. *Nat. Neurosci.* 3, 1266–1273.
- Yamazaki, T., and Tanaka, S. (2009). Computational models of timing mechanisms in the cerebellar granular layer. *Cerebellum* 8, 423–432.
- Yang, Y., and Lisberger, S.G. (2010). Learning on multiple timescales in smooth pursuit eye movements. *J. Neurophysiol.* 104, 2850–2862.
- Yang, Y., and Lisberger, S.G. (2014). Purkinje-cell plasticity and cerebellar motor learning are graded by complex-spike duration. *Nature* 510, 529–532.

**Neuron, Volume 92**

**Supplemental Information**

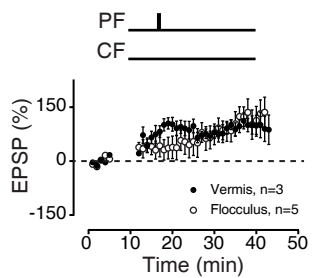
**Timing Rules for Synaptic Plasticity**

**Matched to Behavioral Function**

**Aparna Suvrathan, Hannah L. Payne, and Jennifer L. Raymond**

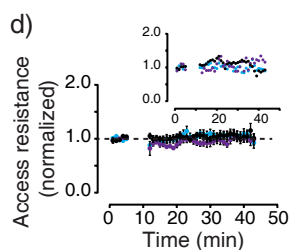
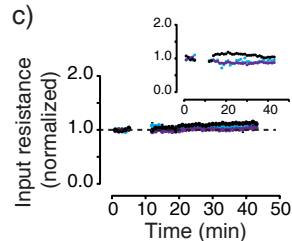
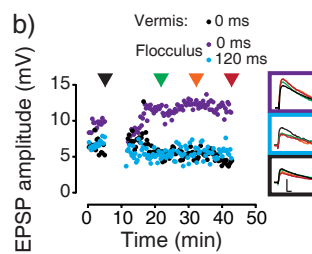
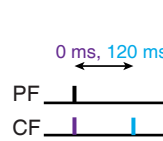
# FIGURE S1

S1A

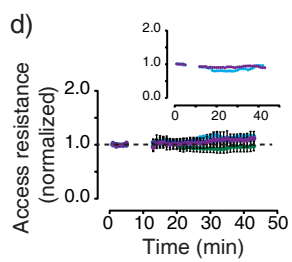
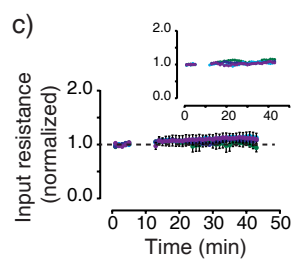
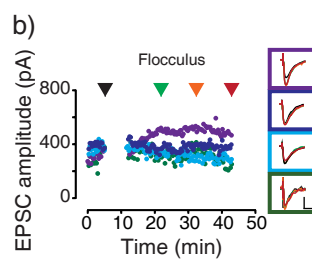
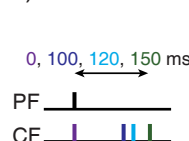


S1C

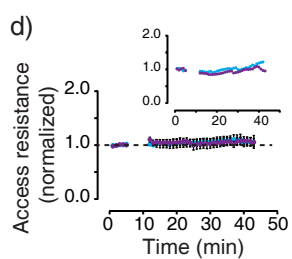
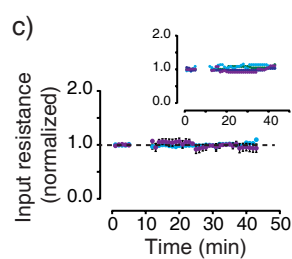
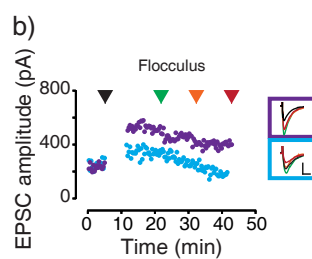
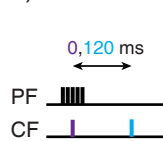
i.



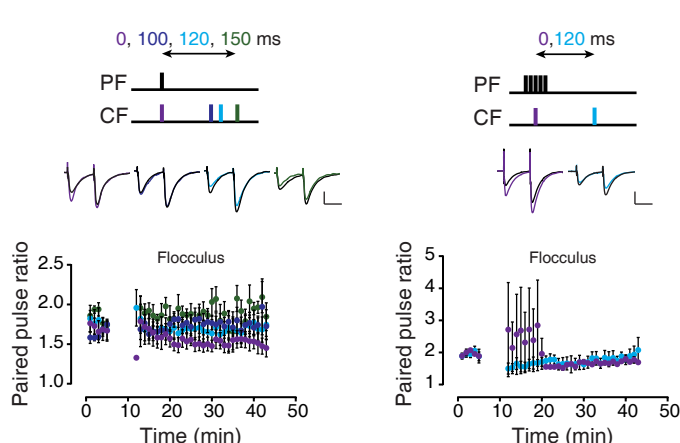
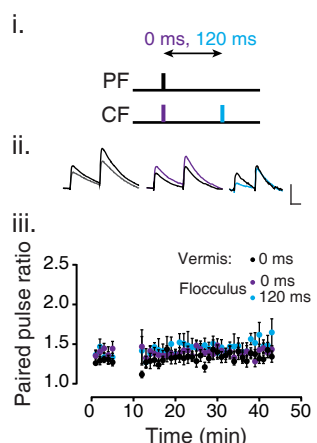
ii.



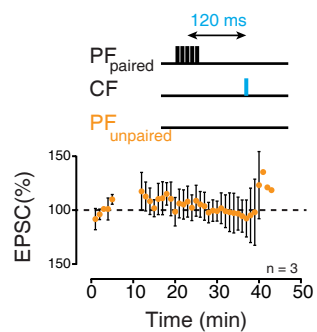
iii.



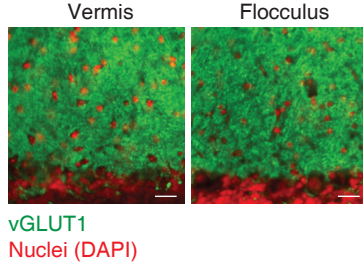
S1D



S1E



S1F



## Supplemental Figure Legends

### Supplemental Figure 1 (related to Figure 1)

**Fig. S1A. Parallel fiber stimulation alone induced LTP in both the vermis and the flocculus.** Non-associative plasticity was induced by PF stimulation alone (300 times at 1Hz, *top schematic*), in both the vermis and the flocculus. n = number of cells, mean  $\pm$  S.E.M.

**Fig. S1B. Estimated climbing fiber delays in flocculus of mouse.**

The delay between retinal image motion, which signals an oculomotor performance error, and climbing fiber responses in the mouse flocculus was estimated using the same analysis used previously in nonhuman primates (Raymond and Lisberger, 1998). Climbing fiber firing was inferred from the complex spikes recorded from Purkinje cells during optokinetic reflex adaptation (Goossens et al., 2004). The phase of the climbing fiber response relative to the visual stimulus ( $\theta$ ) was fit with a fixed delay:

$$\theta = R + 2\pi f T$$

where  $T$  is the climbing fiber delay,  $f$  is the frequency of the stimulus and  $R$  is a constant reference point on the visual stimulus. The best fit to the data was obtained with a value of 121 ms for the delay,  $T$ , and a value of 19.6° for  $R$ . The estimated delay in mice is very similar to the 122 ms delay estimated in nonhuman primates, which supported the prediction that it would be optimal for climbing fiber activity to induce plasticity at synapses active ~122 ms earlier (Raymond & Lisberger, 1998). (See Supplemental Procedures for more details.)

**Fig. S1C. Long-term depression of parallel fiber-to-Purkinje cell synapses is induced by a PF-CF pairing interval of 120 ms and not 0 ms: example cells, and measurements of input and access resistance.**

i) **Long-term plasticity measured in current clamp (related to Fig. 1A, B).** **a)** Schematic showing PF-CF interval, corresponding colors are used in *b-d*. **b)** Example cells for each condition tested. *Inset, right:* Traces showing individual EPSPs for each example cell, boxed in corresponding color. Traces were measured at times indicated by the *colored arrowheads - Black*: at min. 4-5 before the induction of plasticity; *green*: at min. 8-10 after induction of plasticity; *orange*: min. 18-20; *red*: min. 28-30. Scale bars: 5 mV, 20 ms. **c)** Input resistance, normalized to baseline, for all cells used for analysis of LTD measured in current clamp in Fig. 1A, B. *Inset:* input resistance for example cells shown in *b*. **d)** Access resistance, normalized to baseline, for all cells used for analysis of LTD measured in current clamp in Fig. 1A, B. *Inset:* access resistance for example cells shown in *b*.

ii) **Long-term plasticity measured in voltage clamp (related to Fig. 1C).** **a)** Schematic showing PF-CF interval, corresponding colors are used in *b-d*. **b)** Example cells for each PF-CF pairing interval. *Inset, right:* traces showing individual EPSCs for each example cell, boxed in corresponding color, measured at times indicated by the colored arrowheads as in Fig. S1Cib. Scale bars: 200 pA, 20 ms. **c)** Input resistance for all cells shown in Fig. 1C. *Inset:* input resistance for example cells shown in *b*. **d)** Access resistance for all cells shown in in Fig. 1C. *Inset:* access resistance for example cells shown in *b*.

iii) **Long-term plasticity induced by pairing a train of PF stimuli with the CF stimulus (related to Fig. 1D).** **a)** Schematic showing PF-CF interval, corresponding colors are used in *b-d*. **b)** Example cells for each PF-CF pairing interval. *Inset, right:* traces showing individual EPSCs for each example cell, boxed in corresponding color, measured at times indicated by the colored arrowheads. Scale bars: 200 pA, 20 ms. **c)** Input resistance for all cells shown in Fig. 1D. *Inset:* input resistance for example cells shown in *b*. **d)** Access resistance for all cells shown in Fig. 1D. *Inset:* access resistance for example cells shown in *b*. All panels: mean  $\pm$  S.E.M.

**Fig. S1D. Long-term depression is not accompanied by a change in paired pulse ratio.** **i)** Schematics showing PF-CF interval for each column in Fig. S1D, with different PF-CF intervals identified by color, and corresponding colors used in *ii-iii*. **ii)** Example traces for average data shown below in *iii*, where black = min 5, before plasticity induction, and corresponding color = 30 min after induction. Scale bars: *left*: 5 mV, 50 ms, *middle, right*: 200 pA, 40 ms. **iii)** Average paired pulse ratio for experiments on long-term plasticity. *Left:* Current clamp experiments in the flocculus and the vermis, shown in Fig 1A,B. *Middle:* Voltage clamp experiments in the flocculus, with

plasticity induced by single parallel fiber stimuli paired with climbing fiber stimuli, shown in Fig 1C. *Right:* Voltage clamp experiments in the flocculus, with plasticity induced by pairing trains of parallel fiber stimuli with climbing fiber stimuli, shown in Fig 1D. Mean  $\pm$  S.E.M. LTD in the flocculus, induced using both single parallel fiber stimuli and trains, appeared to be expressed post-synaptically, as previously described for cerebellar LTD (Chung et al., 2003; Linden, 2012), since there was no change in the paired-pulse ratio.

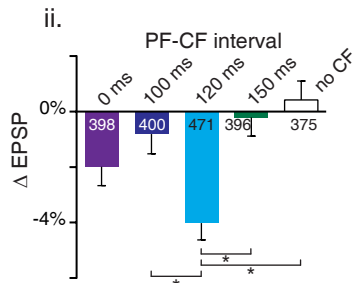
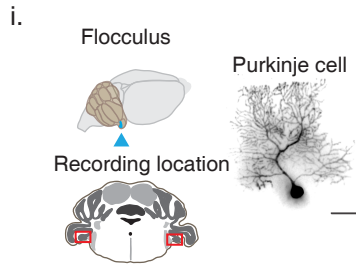
**Fig. S1E. Long-term depression was not expressed in an unpaired control pathway.** For long-term plasticity experiments shown in Fig. 1D, two parallel fiber pathways were stimulated for some cells recorded in the flocculus. One pathway was paired with climbing fiber stimulation ( $\text{PF}_{\text{paired}}$ ), while the other pathway was not paired with CF stimulation ( $\text{PF}_{\text{unpaired}}$ ). The amplitude of the EPSC elicited by stimulation of each PF pathway was tested in an interleaved fashion, before and after pairing of  $\text{PF}_{\text{paired}}$  with CF stimulation (300 times at 1 Hz). No LTD was induced in the  $\text{PF}_{\text{unpaired}}$  pathway. n = number of cells, mean  $\pm$  S.E.M.

**Fig. S1F. Similar staining of parallel fiber synapses, marked by VGLUT1, in slices of vermis and flocculus.** Parallel fiber synapses were stained with an antibody against VGLUT1 (green), and nuclei were stained with DAPI (red), both pseudocolored, in sagittal slices of the cerebellar vermis and coronal slices of the cerebellar flocculus. Scale bar is 20  $\mu\text{m}$ .

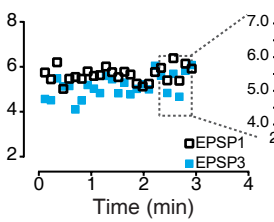
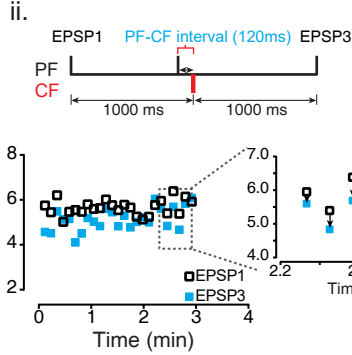
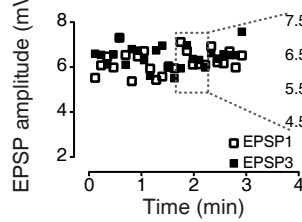
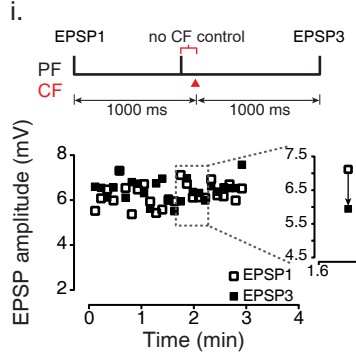
# FIGURE S2

4

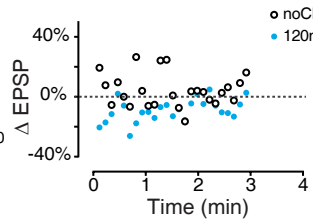
## S2A



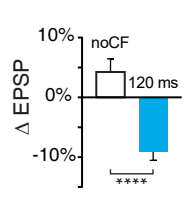
## S2B



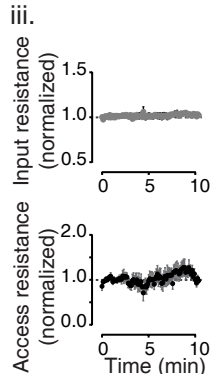
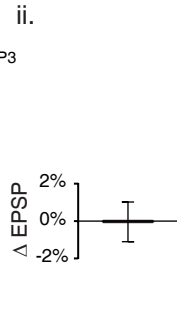
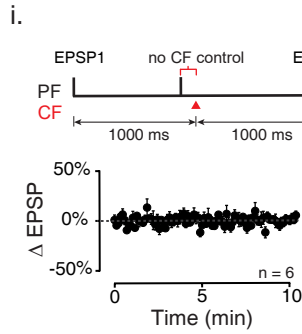
iii.



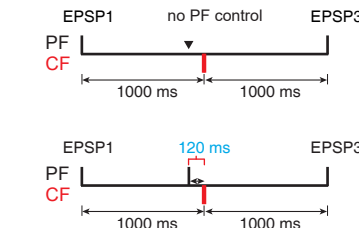
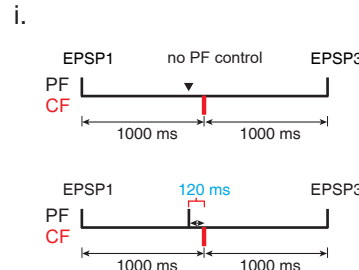
iv.



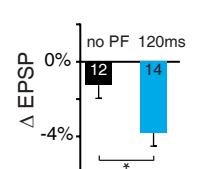
## S2C



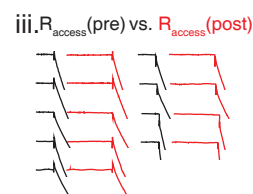
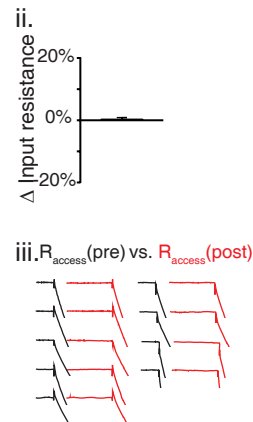
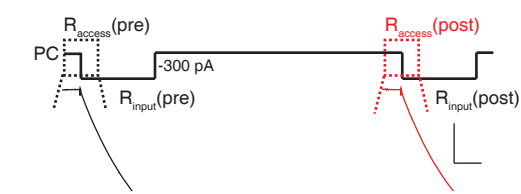
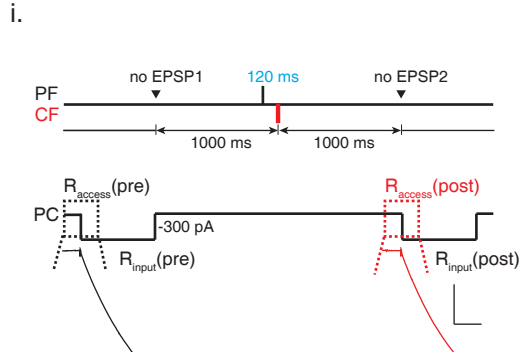
## S2D



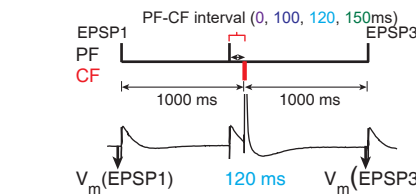
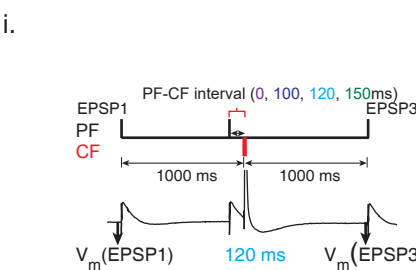
ii.



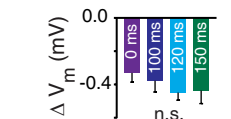
## S2E



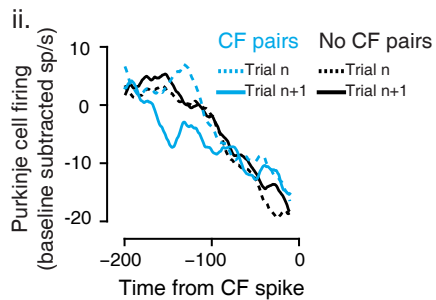
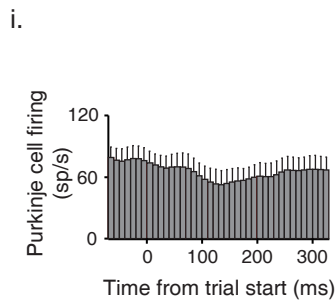
## S2F



ii.



## S2G



**Supplemental Figure 2** (related to Figure 2)

**Fig. S2A. Single-trial plasticity in the flocculus, analyzed by averaging across trials rather than across cells shows the most depression at a PF-CF interval of 120 ms.** **i)** Top left: Flocculus shown in blue (arrowhead). Bottom left: Recording location in a coronal plane (red boxes). Right: Dye-filled Purkinje cell from the flocculus, scale bar 20  $\mu$ m. Maximum-intensity projection of Z-stacks. Gamma-filtering was used on each image of a Z-stack to compensate for differences in absolute intensity along the depth of the slice (see Supplemental Procedures). **ii)** Single-trial data from the flocculus, shown in Fig. 2B, analyzed by pooling the 19-25 trials at each PF-CF interval for each cell, across all cells and then averaging, instead of using a single average value for each PF-CF interval for each cell. \*  $p < 0.05$ , one way ANOVA on ranks followed by Dunn's pairwise comparison, n = number of trials, mean  $\pm$  S.E.M.

**Fig. S2B. Single trial plasticity in the flocculus: example cell.** **i, ii)** Measurement of single-trial plasticity is illustrated in one example cell in the flocculus. *Top schematics* illustrate experimental design, where PF stimulation was either presented alone (*i, no CF*; red arrowhead indicates omitted CF stimulus), or paired with CF stimulation (*ii, 120 ms PF-CF interval*). The amplitudes of EPSP1 (open black squares) and EPSP3 (filled black, filled blue) from each of 25 consecutive trials are plotted, to show the fluctuations in EPSP amplitude. (*i*) For the no CF control, there was no consistent difference between EPSP1 and EPSP3. *Inset*: Expanded section showing both increases and decreases from EPSP1 to EPSP3 on individual trials. (*ii*) For a PF-CF pairing interval of 120 ms, the EPSP was consistently smaller post-pairing (EPSP3, blue), as compared with pre-pairing (EPSP1, open squares), illustrated in the expanded inset section. **iii)** The  $\Delta$ EPSPs (EPSP1 to EPSP3) measured on the individual trials tended to show more depression for a PF-CF pairing interval of 120 ms, than those measured during the no CF control trials (open symbols). **iv)** Averages across trials for the data shown in *iii*. \*\*\*\*  $p < 0.00001$ , t-test, mean  $\pm$  S.E.M.

**Fig. S2C. PF EPSPS were stable if not paired with a CF** **i)** The change in parallel fiber-to-Purkinje cell EPSP amplitude ( $\Delta$ EPSP) on each trial was measured in the flocculus, during the no-CF control condition (red arrowhead indicates omitted CF stimulus) used for the single-trial plasticity experiments (*top schematic*), and there was no change over time. **ii)** Averaged over more than 10 min, the  $\Delta$ EPSP was close to zero. **iii)** Associated changes in input resistance and access resistance for these cells (See Supplemental Experimental Procedures). n = number of cells, mean  $\pm$  S.E.M.

**Fig. S2D. CF alone (no PF) controls, in the flocculus.** **i)** Schematic of experimental design. *Top*: In the no-PF control trials, the CF activation was delivered without paired PF activation (arrowhead indicates omitted PF stimulus). *Bottom*: In other trials, the CF was paired with the PF at a 120 ms delay. **ii)** A PF-CF interval of 120 ms induced single trial depression, as in the cells in Fig. 2B, which was significantly greater than that observed in the no-PF control condition, \*  $p < 0.05$ , t-test, mean  $\pm$  S.E.M.

**Fig. S2E. PF-CF pairing does not induce a change in input or access resistance.** **i)** Schematic of experimental design. The PF stimuli used to measure single-trial depression (EPSP1 and EPSP3) before and after a PF-CF pairing at 120 ms, were replaced by a hyperpolarizing current step, in order to assess changes in input and access resistance. **ii)** There was no change in input resistance (black bar, mean  $\pm$  S.E.M., n = 10 cells) after PF-CF pairing at 120 ms. **iii)** There was no change in access resistance induced by PF-CF pairing at 120 ms. Bridge-balanced responses to hyperpolarizing current steps are shown for all 10 cells before (black) and after (red) PF-CF pairing, mean  $\pm$  S.E.M.

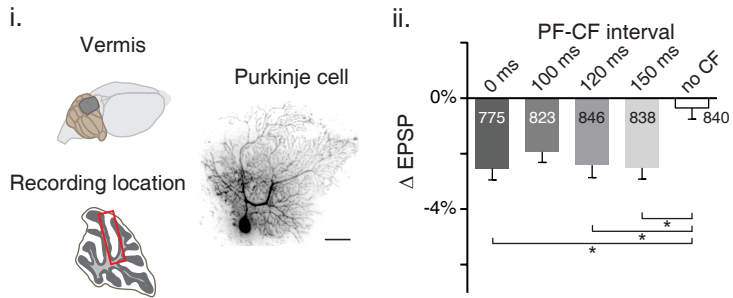
**Fig. S2F. Changes in membrane voltage do not underlie selective depression at a PF-CF interval of 120 ms in the flocculus.** **i)** Example trace showing measurement of membrane potential ( $V_m$ ) just prior to the measurements of the PF-to-PC EPSPs, before (EPSP1) and after (EPSP3) a PF-CF pairing. These measurements were used to calculate  $\Delta V_m = V_m(\text{EPSP3}) - V_m(\text{EPSP1})$  for each trial in the single-trial plasticity experiments shown in Fig. 2B. **ii)** There was no difference in  $\Delta V_m$  across the different PF-CF pairing intervals. For all cells shown in Fig. 2B, the mean  $\Delta V_m$  was less than 0.5 mV, and was indistinguishable across different PF-CF intervals. Mean  $\pm$  S.E.M.

**Fig. S2G. Raw firing rates for *in vivo* trial-by-trial analysis.** **i)** Mean Purkinje cell firing rates for cells used in Fig. 2C, aligned to trial start. **ii)** Baseline-subtracted Purkinje cell firing rates used for Fig. 2C. *Blue* = CF pairs: pairs of trials where there was a climbing fiber spike on the first trial and not on the second. *Black* = No-CF pairs, where there was no climbing fiber spike on either trial. Dotted lines show the mean for the first trials, and continuous lines show the mean for the second trials, aligned to the time of the climbing fiber spike (for more detail, including alignment of No-CF pairs, see Supplemental Experimental Procedures), mean  $\pm$  S.E.M. The *in vivo* plasticity shown in Figure 2C could, in principle, reflect changes at the PF-to-PC synapses or any of several other synaptic sites (Mittmann and Häusser, 2007), but the similar timing for the single-trial plasticity at the PF-to-PC synapses (Figure 2B) makes it a candidate mechanism for the *in vivo* changes.

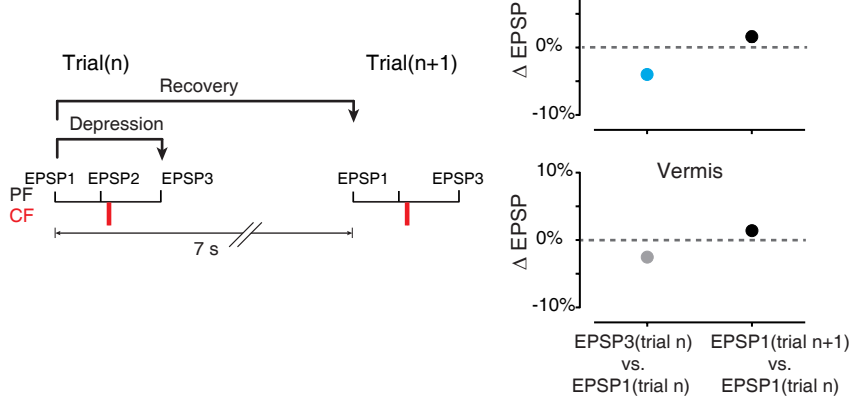
FIGURE S3

7

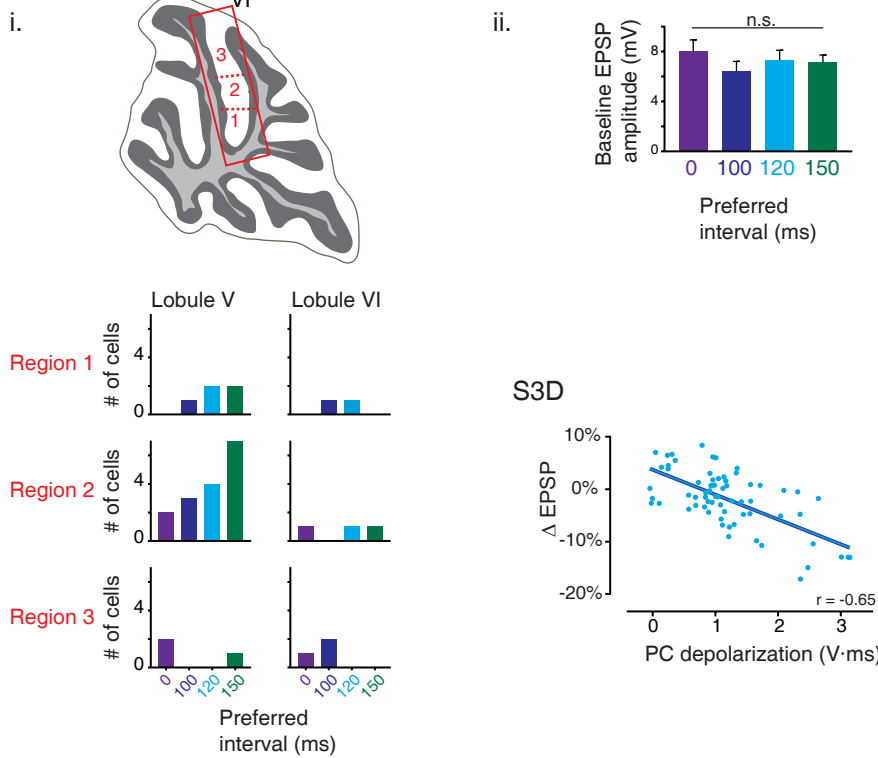
## S3A



## S3B



## S3C



**Supplemental Figure 3** (Related to Figure 3)

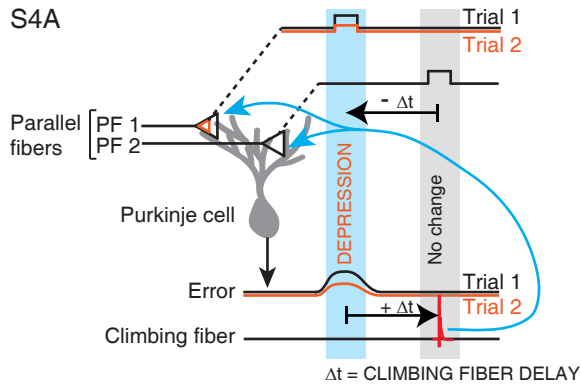
**Fig. S3A. Single-trial plasticity analyzed by averaging across trials rather than across cells confirms that depression was not tuned to a single PF-CF interval in the vermis.** **i)** *Top left:* Lobules V-VI of vermis, shown in grey. *Bottom left:* Recording location illustrated in the parasagittal plane (red box). *Right:* Dye-filled Purkinje cell from the vermis, scale bar 20  $\mu$ m. Maximum-intensity projection of Z-stacks. Gamma-filtering was used on each image of a Z-stack to compensate for differences in absolute intensity along the depth of the slice (see Supplemental Procedures). **ii)** Single-trial data from the vermis, shown in Fig. 3A, analyzed by pooling the 19-25 trials at each PF-CF interval for each cell, across all cells and averaging, instead of using a single average value for each PF-CF interval for each cell. \*  $p < 0.05$ , one way ANOVA on ranks followed by Dunn's pairwise comparison,  $n$  = number of trials, shown inside bars, mean  $\pm$  S.E.M.

**Fig. S3B. Single-trial depression of PF-to-PC synapses recovers between trials.** *Left:* Schematic illustrating the analysis for measuring single-trial synaptic depression, and recovery from one trial to the next. *Right:* A single PF-CF pairing at an interval of 120 ms in the flocculus (*top*) and 0 ms in the vermis (*bottom*) decreased the amplitude of the EPSP elicited in the Purkinje cells by PF stimulation after pairing, as compared with before pairing (EPSP3(trial n) vs. EPSP1(trial n); *grey or light blue*; re-plotted from Fig S2Aii and S3Aii). However, the EPSP amplitude recovered by the beginning of the next trial (*black*, EPSP1(trial n+1) vs. EPSP1(trial n)), which was 6 s after the PF-CF pairing, since the time from the start of one trial to the next was 7 s.  $n = 774$  trials from 470 trials from 19 cells in flocculus and 31 cells in vermis. Mean  $\pm$  S.E.M., error bars smaller than symbol size.

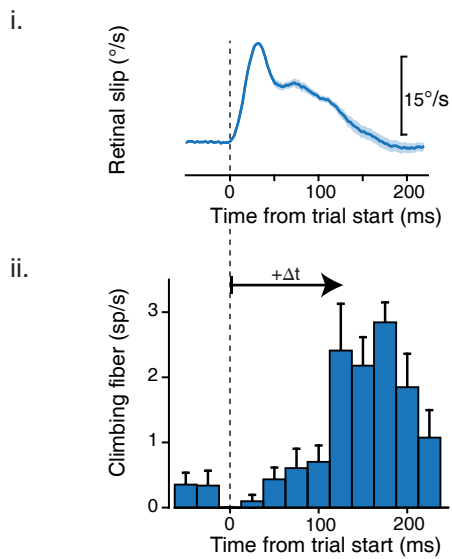
**Fig. S3C. PF-CF interval that induces maximum single-trial depression in the vermis was not related to spatial localization or EPSP amplitude.** **i)** Cells shown in Fig. 3 were recorded from lobules V and VI of slices of the vermis. *Top cartoon* shows a parasagittal slice of vermis divided into three regions. *Below:* Number of cells recorded from each region, plotted according to preferred PF-CF interval: 0 ms (*purple*), 100 ms (*dark blue*), 120 ms (*light blue*) or 150 ms (*green*). There was no clear organization of cells that preferred different PF-CF intervals by region within lobules V and VI. **ii)** Baseline EPSP amplitude was not different between cells which preferred different PF-CF intervals (repeated measures ANOVA on ranks), mean  $\pm$  S.E.M.

**Fig. S3D. Single-trial plasticity was correlated with PC depolarization in the flocculus.** For flocculus Purkinje cells shown in Fig. 2B, single-trial synaptic depression ( $\Delta$ EPSP) in each cell, for each PF-CF interval, was correlated with the amount of Purkinje cell depolarization, as shown for vermis in Fig 3E (See Fig. 3C and Supplemental Experimental Procedures for how Purkinje cell depolarization was measured).

**FIGURE S4**



S4B



**Supplementary Figure 4** (related to Fig. 4)

**Fig. S4. Error signals carried by climbing fibers are delayed relative to motor performance errors.**

**A)** The activity of some parallel fibers (PF1) contributes to a motor error on Trial 1. The error elicits a spike in the climbing fiber at a delay,  $\Delta t$ , relative to the activity of the parallel fibers that contributed to the error. Synapses that contributed to the motor error (PF1) are selectively depressed by the climbing fiber. Parallel fiber synapses active at the same time as the climbing fiber spike (PF2) did not contribute to the error, and are not depressed by the climbing fiber. Thus, climbing fiber-triggered plasticity compensates for the delay ( $\Delta t$ ) in the error signals carried by the climbing fibers, by inducing depression of the parallel fiber synapses that were active at a time,  $-\Delta t$ , before the climbing fiber spike, providing a mechanism for solving the temporal credit assignment problem.

**B i)** During vestibulo-ocular reflex (VOR) learning (Fig. 2C, D), image motion on the retina (retinal slip) indicates a performance error. VOR learning was induced by pairing a step of constant head velocity with motion of a visual stimulus (Kimpo et al., 2014; see Supplemental Experimental Procedures). Under such conditions, the eye movements fail to stabilize images on the retina, i.e., there is retinal slip, especially in the early part of the combined visual-vestibular stimulus, before visually-driven eye movements begin to compensate for an inadequate VOR.

**ii)** The retinal slip signaling an error is encoded by the climbing fibers, with firing delayed  $>100$  ms (*arrow,  $+\Delta t$* ), relative to the onset of image motion ( $t = 0$ ). Previous work has shown that when the timing of the error is precise, the timing of the climbing fiber response is also precise (Raymond and Lisberger, 1998), consistent with the more general role of the cerebellum in precise timing (Ivry and Spencer, 2004). In the specific VOR learning task used for the present analysis, the error is extended in time, and therefore the climbing fiber responses are also extended in time. We leveraged the trial-to-trial variation in the climbing fiber spike times to show that for each trial, the plasticity is precisely timed relative to each climbing fiber spike, rather than to some other task-related variable.

## Supplemental Experimental Procedures

All protocols were approved by the Stanford Administrative Panel on Laboratory Animal Care.

### *In vitro* slice electrophysiology.

Adult male C57Bl/6 mice (21-35 days) from Charles River Laboratories were used for all cerebellar slice recordings. Mice were kept on a 12 hour inverted day/night cycle and had *ad libitum* access to food and water. For cerebellar slice experiments, animals were anesthetized with isoflurane, cervically dislocated, and decapitated. The brain was extracted, and dissected under ice-cold artificial cerebrospinal fluid (aCSF (concentration in mM): NaCl(119), KCl(2.5), NaH<sub>2</sub>PO<sub>4</sub>(1), NaHCO<sub>3</sub>(26.2), MgCl<sub>2</sub>(1.3), CaCl<sub>2</sub>(2.5), D-Glucose(10), equilibrated with Carbogen (95% O<sub>2</sub>, 5% CO<sub>2</sub>, Praxair)). 300 µm slices were made using a Leica VT1200 Vibrating Microtome. Because the cellular organization of the flocculus is rotated relative to the vermis (Fujita et al., 2012, 2014), the vermis was sliced parasagittally, and the flocculus coronally, in order to cut in a plane orthogonal to the parallel fibers, and parallel to the Purkinje cell dendrites (Fig. S2Ai, S3Ai). Slices were allowed to recover at 35°C for 30 min, and then at room temperature for 1 hour.

Slices were incubated in a recording chamber on an Olympus BX51WI upright microscope, in artificial cerebrospinal fluid maintained at 30-32°C. Purkinje cells were visualized with differential interference contrast optics, and recording was done in the whole-cell configuration. Stimulation was done using bipolar stimulating electrodes made from theta glass (Sutter Instruments), which were positioned in the outer third of the molecular layer in order to stimulate parallel fibers (PFs), and in the granule cell layer close to the Purkinje cell body in order to stimulate climbing fibers (CFs).

Patch electrodes (3-6 MΩms) were pulled from borosilicate glass tubing (Harvard Apparatus) and filled with an internal solution containing (concentration in mM): KMeSO<sub>4</sub>(133), KCl(7.4), MgCl<sub>2</sub>(0.3), HEPES(10), EGTA(0.1), MgATP(3), Na<sub>2</sub>GTP(0.3), pH adjusted to 7.3 with KOH, osmolarity 260-290 mOsm. 100 µM picrotoxin was added to the aCSF to block GABA<sub>A</sub> channels. Cells were held in voltage clamp at -70 mV or in current clamp. Signals were acquired at 20 kHz using a Multiclamp 700B amplifier and low-pass filtered at 10 kHz. Access resistance was < 25 MΩms and both input and access resistance were monitored for stability throughout the recording.

All aCSF reagents and picrotoxin were obtained from Sigma-Aldrich, except NaCl (both from Sigma-Aldrich and from AMD chemicals) and KOH, which was obtained from AMD chemicals. Slice physiology data were analyzed in pCLAMP 10 (Clampfit) or MATLAB, with statistical tests performed using SigmaPlot or GraphPad Prism (see section on Statistics).

### Long-term plasticity *in vitro*.

Long term plasticity at parallel fiber-to-Purkinje cell (PF-to-PC) synapses was induced by parallel fiber-climbing fiber (PF-CF) pairings repeated 300 times at 1 Hz, delivered ≤15 minutes after whole-cell recording began. Parallel fiber and climbing fiber stimuli were each 150 µs long. Each climbing fiber stimulus was paired with an individual parallel fiber stimulus, or a brief train of five parallel fiber stimuli at 100 Hz. These stimulation procedures are commonly used in studies of cerebellar LTD, and thus facilitate comparison with previous findings (Coesmans et al., 2004; Hansel and Linden, 2000; Wadiche and Jahr, 2005; Wang et al., 2000).

The interval between the parallel fiber and climbing fiber stimuli (PF-CF interval) varied across experiments (0, 100, 120 or 150 ms). When a parallel fiber train was paired with the climbing fiber, the PF-CF interval was measured from the middle of the parallel fiber train, except in one cell where it was measured from the second pulse in the train. Cells were held in current clamp during the induction of plasticity to permit climbing fiber-driven complex spikes (Hansel et al., 2006; Sarkisov and Wang, 2008).

Before and after pairing, the strength of PF-to-PC synapses was tested with parallel fiber stimulation at 0.05 Hz. In some experiments, cells were held in current clamp during testing; and in some experiments, the cells were held in voltage clamp (-70mV) during testing. In the long-term current clamp recordings, capacitance was compensated, bridge was balanced, and sufficient current (<1 nA) was injected for an initial baseline membrane voltage between -69 and -75 mV. In a subset of the voltage clamp recordings, series resistance was compensated. Series and input resistance were monitored, and changed by <20% throughout the recording. EPSP or EPSC amplitude was measured in Clampfit.

Measurements of input and access resistance (Supplemental Figures S1C; S2C) were obtained from the response to a hyperpolarizing current or voltage step delivered after every EPSP/EPSC measurement, measured in Clampfit. All EPSP and EPSC example traces shown in all figures were low-pass filtered at 500 Hz, and stimulus artifacts were truncated.

### **Single-trial plasticity *in vitro*.**

Short-term plasticity induced by a single PF-CF pairing was characterized in slices from the flocculus and vermis. In these experiments, each trial consisted of a single pairing of parallel fiber and climbing fiber stimulation, plus two tests of the synaptic response to the parallel fiber stimulation alone. The parallel fiber stimulation that was paired with climbing fiber stimulation (Fig. 2A, PF EPSP2) was delivered at 0 ms (i.e. coincident with), 100 ms, 120 ms or 150 ms before climbing fiber stimulation. The test pulses were delivered to the parallel fibers 1 s before and 1 s after climbing fiber stimulation (Fig. 2A, PF EPSP1 and PF EPSP3), and these measurements were used to calculate the percent change in EPSP amplitude for that trial. For the analyses in Fig. 2B and 3A, B, the change in the EPSP measured on all trials of a given type (PF-CF pairing interval or control) in one cell were averaged, and then each cell contributed a single average value for the change in the EPSP. For Fig S2A and S3A, all trials across all cells, for a given PF-CF interval, were pooled and then averaged. Initial baseline membrane voltage was between -60 mV and -75 mV, as for LTD studies (Coesmans et al., 2004; Hansel et al., 2006) (<1nA injected).

Parallel fiber and climbing fiber stimulus pulses were 150  $\mu$ s long. Parallel fibers were activated with one pulse. Climbing fibers were activated with two stimulus pulses, 10 ms apart. Two stimuli were delivered to climbing fibers in order to broaden the complex spike, because *in vivo*, single trial plasticity is observed only on trials when the width of the complex spike is broad (Yang and Lisberger, 2014). Climbing fibers are known to transmit brief, high-frequency bursts of ~10 ms in duration, and it has been shown that stimulation of the climbing fibers with a 10-ms train rather than a single pulse broadens the complex spike and increases the probability of LTD (Mathy et al., 2009; see also Rasmussen et al., 2013). Paired stimulation of parallel fibers and climbing fibers was done in current clamp to allow depolarization during the climbing fiber-triggered complex spike, which is necessary for induction of plasticity.

The same cells were tested with PF-CF pairing intervals of 0, 100, 120, and 150 ms, as well as with control trials in which the PF-CF pairing was replaced with a single stimulus to the PF alone or the CF alone. For the “No CF” control condition, three parallel fiber stimuli were given at the same time points as in the 120 ms PF-CF interval condition, but without the CF stimulation. Each cell underwent 19–25 trials at each PF-CF interval. Trials with the same PF-CF pairing interval were delivered in blocks of 10–25 trials, with trial start times 7 s apart. Blocks were presented in pseudorandom order.

We quantified the extent to which the Purkinje cell depolarized during the complex spike as the area under the curve (Fatt and Katz, 1951) of the Purkinje cell voltage during the complex spike (Fig. 3C), a measure similar to charge transfer measured in voltage clamp (Arenz et al., 2008). The area under the complex spike waveform was measured in a 150 ms window after the climbing fiber stimulus, relative to the baseline membrane potential immediately prior to PF-EPSP 2 (see Fig. 3C for schematic showing measurement area). If, during the 150 ms analysis window, there was post-complex spike hyperpolarization below the baseline, the area of the hyperpolarization was subtracted from the area of the depolarization.

The tuning of single trial plasticity for the PF-CF interval was quantified with a Selectivity Index (SI), calculated as  $SI = (\text{Depression at preferred interval} - \text{Average depression at the three non-preferred intervals}) / \text{Depression at preferred interval}$  (Van Hooser, 2005). Cells that exhibited <1% depression at the preferred interval were excluded from the calculation of the selectivity index to avoid spuriously high selectivity indices (Mazurek et al., 2014). A selectivity index of zero indicates no difference in the amount of depression induced by the different PF-CF pairing intervals tested, i.e. equal depression at all intervals, whereas a selectivity index of 1.0 indicates depression at the preferred interval and no depression, on average, at non-preferred intervals. A selectivity index greater than 1.0 is also possible if there is potentiation, rather than depression, at the non-preferred intervals.

### **Statistics.**

For all statistical analyses, a D'Agostino-Pearson test for normality was performed to determine whether a parametric or non-parametric test should be performed. For current- and voltage-clamp measurement of long-term plasticity (Fig. 1B, 1D), significance was assessed using a Mann-Whitney test. Long-term plasticity induced by different PF-CF intervals (Fig. 1C) was compared using a Kruskall-Wallis ANOVA on ranks, followed by a Dunn's pairwise comparison. Single-trial data from the flocculus (Fig. 2B) were analyzed using a repeated measures ANOVA on ranks, followed by a post-hoc Student-Neuman-Keuls pairwise comparison. Single-trial data from the vermis (Fig. 3A) were analyzed using a repeated measures ANOVA, followed by a post-hoc Student-Neuman-Keuls pairwise comparison. Selectivity index data in Fig. 3F were compared using a Mann-Whitney test. Single-trial data in Supplemental figures S2A, S3A were analyzed using a Kruskall-Wallis ANOVA on ranks followed by Dunn's pairwise comparison. Comparison of the no-CF vs. 120 ms PF-CF pairing trials for an example cell (Fig. S2B iv), and comparison of the summary data for CF-alone control trials vs. 120 ms PF-CF interval trials (Fig. S2D ii) were

each done with a Student's t-test. Comparison of membrane potential across PF-CF intervals (Fig. S2F) was performed with a repeated measures ANOVA, and comparison of baseline EPSP amplitude across different cells in the vermis (Fig. S3C ii) was done with a Kruskall-Wallis ANOVA on ranks. Statistical tests were done in GraphPad Prism, except for ANOVAs with post-hoc measurements, which were done using SigmaPlot.

### **Single trial *in vivo* plasticity.**

Previously published data (Kimpo et al., 2014) from two awake, behaving, male rhesus monkeys were reanalyzed to align trial-to-trial changes in Purkinje cell simple spike firing rates and eye movements to the time of the associated climbing fiber spike. Extracellular recordings were made of the simple spikes and complex spikes of isolated Purkinje cells during vestibulo-ocular reflex (VOR) gain-increase training, which paired vestibular stimuli (head turns) with image motion in the opposite direction. The vestibular stimuli (250 ms or 500 ms steps of head velocity at 15°/s) were delivered by passive rotation of the animal about an earth-vertical axis. Visual stimuli consisted of a projected black-and-white pattern with a small central fixation target, and moved in the opposite direction from the vestibular stimulus at 15°/s. Horizontal eye position (relative to the head) was measured using the eye coil method (Robinson, 1963), and was converted to eye velocity using a hardware differentiator and 300 Hz low-pass filter. Large saccades were identified using an automatic velocity threshold algorithm, and the corresponding eye velocity data excluded from the analysis. Remaining small saccades were removed manually. If more than 50 ms of a trial was marked by a saccade, the entire trial was excluded from the analysis.

Single units were recorded extracellularly in the flocculus and ventral paraflocculus using platinum-iridium electrodes. The cells included in the analysis were all identified as horizontal gaze velocity Purkinje cells (Raymond and Lisberger, 1998). Since spikes in a climbing fiber elicit a characteristic complex spike in their Purkinje cell targets in a one-to-one manner (Eccles et al., 1966), the complex spikes provide a readout of spikes in the climbing fiber input, hence we refer to a complex spike as a "climbing fiber spike." Simple spikes and complex spikes were identified as described previously (Kimpo et al., 2014) and Purkinje cell output firing rates were calculated using the reciprocal interval method (Lisberger and Pavelko, 1986). VOR learning trials were sorted according to whether or not there was a climbing fiber spike in the window 75-250 ms after onset of the visual-vestibular stimulus. Each pair of consecutive trials in which there was a climbing fiber spike on the first trial, but not on the second trial was classified as a CF trial pair. Each pair of consecutive trials in which there was no climbing fiber spike on either trial was classified as a No CF trial pair. The Purkinje cell firing in the first trial was then subtracted from that in the second trial to obtain the trial-to-trial changes in firing rate. The trial-to-trial changes in firing for each CF trial pair were aligned to the time of the climbing fiber spike and then averaged (Fig. 2C). The trial-to-trial changes in firing for the No CF trial pairs were aligned on randomly selected times of a climbing fiber spike from the CF trial pairs (both trials of a No CF pair aligned on the same time), so that the populations of CF and No CF trial pairs were aligned to the same distribution of climbing fiber spike times from within the 75-250 ms analysis window. Similarly, eye velocity during the first trial in a pair was subtracted from that in the second trial to obtain the trial-to-trial changes in behavior (Fig. 2D). Negative values (Fig. 2D) indicate eye movement in the direction opposite to head rotation, so that a more negative value represents an adaptive increase in VOR amplitude. Trial-to-trial changes in Purkinje cell firing rate and eye velocity were analyzed in MATLAB (Mathworks Inc.). Trial-to-trial changes were first averaged across trials within a cell, and Purkinje cell firing rates were smoothed with a 25 ms sliding average window. Finally, data were averaged across cells (n=9) for each condition.

Trial-to-trial changes were only analyzed for times preceding the climbing fiber spike by more than 10 ms, due to artifacts caused by smoothing of the typical post-complex spike pause in simple spike firing. Bootstrapping was used to assess significance of changes in Purkinje cell firing rates and eye velocity. For each cell, pairs of consecutive trials were randomly selected from the pool of all consecutive trials, to match the quantity of CF trial pairs that were included in the average for that cell. Average trial-to-trial changes were then calculated and averaged for each cell as described above, and a grand average for all cells was determined. This process was repeated 1000 times to create a bootstrapped distribution for both firing rate and eye velocity. Observed trial-to-trial changes in Purkinje cell firing rates and eye velocity were determined to be significant if they exceeded the 95% confidence intervals of each bootstrapped distribution (dashed lines in Fig 2C and D).

### **Estimation of climbing fiber delay in mice.**

For the analysis in Supplemental Fig. S1A, climbing fiber responses during optokinetic reflex adaptation in mice (Goossens et al., 2004) were analyzed to estimate climbing fiber delays using the same method previously used to estimate the delays in the error signals carried by the climbing fibers during oculomotor learning in monkeys (Raymond and Lisberger, 1998). The phase of peak climbing fiber firing relative to the optokinetic stimulus was first calculated from the published mouse data (Goossens et al., 2004) by adding together complex spike phase

relative to eye, with eye phase relative to the optokinetic stimulus. The phase of climbing fiber firing relative to the optokinetic stimulus exhibited a progressive lag with increase in stimulus frequency from 0.1 Hz to 0.8 Hz. This phase lag was fit with a fixed delay by fitting the equation:  $\theta = R + 2\pi f T$ , where  $\theta$  is the phase of the climbing fiber firing relative to the visual stimulus,  $T$  is the predicted climbing fiber delay,  $f$  is the frequency of the training stimulus and  $R$  is a constant reference point on the visual stimulus. This yielded an estimate of 121 ms for the climbing fiber delay ( $T$ ) in mouse Purkinje cells, a value similar to the 122 ms estimated in monkeys. Published data for a 0.05 Hz optokinetic stimulus were excluded from the analysis because of the extremely low amplitude of the climbing fiber response, which would make determination of the phase less certain, and because the measured phase of the climbing fiber firing during the 0.05 Hz optokinetic stimulus lagged rather than led the phase at 0.1 Hz, making it impossible to fit with a delay.

#### **Purkinje cell dye fills.**

100 mM Alexa Fluor-488 hydrazide sodium salt (Life Technologies) was added to the internal solution for dye-fill reconstructions of Purkinje cells. Whole-cell recording using the dye-containing internal solution was maintained for a minimum of 40 min, the pipette slowly retracted, and the slice fixed in 4% formaldehyde in 0.1X PBS. Cells were imaged using a Perkin-Elmer spinning-disk confocal microscopy system on a Zeiss AxioScope body, equipped with a 488 nm laser, a Hamamatsu EMCCD camera, and run by Volocity software. Gamma-filtering was used on each image of a Z-stack to compensate for differences in absolute intensity along the depth of the slice. Maximum-intensity projections of Z-stacks were then obtained using Fiji (ImageJ) software (Schindelin et al., 2012).

#### **Antibody staining.**

Brains from adult male C57 Bl6 mice (28-35 d old) were fixed in 4% formaldehyde in phosphate buffered saline (PBS) and then cryoprotected in buffered sucrose solution (30% in PBS). Immunohistochemistry was carried out on 20 micrometer thick coronal (for the flocculus) or sagittal (for the vermis) sections, made on a Leica CM3050 cryostat. Tissue sections were washed thoroughly in PBS containing 0.1% BSA, blocked in 10% Normal Goat Serum (NGS) containing 0.3% Triton X-100 for 1 hour at room temperature, washed in PBS with 0.1% BSA, and incubated in primary antibody overnight at 4°C. Primary antibody was 1:5000 anti VGLUT1 Guinea pig polyclonal (Millipore AB5905), made in 2% NGS PBS with 0.1% BSA and 0.1% Triton X-100. Tissue sections were then washed, as previously, and incubated in secondary antibody for 1.5 hrs at room temperature. Secondary antibody was goat anti-guinea pig Secondary Antibody, Alexa Flour® 594 conjugate (Invitrogen A-11076) at 1:500 in 2% NGS in PBS with 0.1% Triton X-100. Sections were washed again, as previously, and mounted in Vectashield mounting medium containing DAPI. Images were acquired using a widefield fluorescence microscope system built around a Zeiss Axiovert 200M, equipped with a 100W HBO lamp and an ORCA Flash 4.0 LT sCMOS camera (Hamamatsu). A 10X, 0.3 NA objective was used and the system was controlled using μManager software (Edelstein et al., 2010).

## Supplemental References

- Arenz, A., Silver, R.A., Schaefer, A.T., and Margrie, T.W. (2008). The contribution of single synapses to sensory representation in vivo. *Science* 300, 977–980.
- Chung, H.J., Steinberg, J.P., Huganir, R.L., and Linden, D.J. (2003). Requirement of AMPA receptor GluR2 phosphorylation for cerebellar long-term depression. *Science* 300, 1751–1755.
- Coesmans, M., Weber, J.T., De Zeeuw, C.I., and Hansel, C. (2004). Bidirectional parallel fiber plasticity in the cerebellum under climbing fiber control. *Neuron* 44, 691–700.
- Eccles, J.C., Llinas, R., and Sasaki, K. (1966). The excitatory synaptic action of climbing fibres on the Purkinje cells of the cerebellum. *J. Physiol.* 268–296.
- Edelstein, A., Amodaj, N., Hoover, K., Vale, R., and Stuurman, N. (2010). Computer control of microscopes using manager. *Curr. Protoc. Mol. Biol.* 1–17.
- Fatt, P., and Katz, B. (1951). An analysis of the end-plate potential recorded with an intra-cellular electrode. *J. Physiol.* 115, 320–370.
- Fujita, H., Morita, N., Furuichi, T., and Sugihara, I. (2012). Clustered fine compartmentalization of the mouse embryonic cerebellar cortex and its rearrangement into the postnatal striped configuration. *J. Neurosci.* 32, 15688–15703.
- Fujita, H., Aoki, H., Ajioka, I., Yamazaki, M., Abe, M., Oh-Nishi, A., Sakimura, K., and Sugihara, I. (2014). Detailed expression pattern of aldolase C (aldoc) in the cerebellum, retina and other areas of the CNS studied in aldoc-venus knock-in mice. *PLoS One* 9, e86679.
- Goossens, H.H.L.M., Alphen, A.M. Van, Steen, J. Van Der, Stahl, J.S., Zeeuw, C.I. De, and Frens, M.A. (2004). Simple spike and complex spike activity of floccular Purkinje cells during the optokinetic reflex in mice lacking cerebellar long-term depression. *Neuroscience* 19, 687–697.
- Hansel, C., and Linden, D.J. (2000). Long-Term Depression of the cerebellar climbing fiber–Purkinje neuron synapse. *Neuron* 26, 473–482.
- Van Hooser, S.D. (2005). Orientation Selectivity without Orientation Maps in Visual Cortex of a Highly Visual Mammal. *J. Neurosci.* 25, 19–28.
- Ivry, R.B., and Spencer, R.M.C. (2004). The neural representation of time. *Curr. Opin. Neurobiol.* 14, 225–232.
- Linden, D.J. (2012). A late phase of LTD in cultured cerebellar Purkinje cells requires persistent dynamin-mediated endocytosis. *J. Neurophysiol.* 107, 448–454.
- Lisberger, S.G., and Pavelko, T.A. (1986). Vestibular signals carried by pathways subserving plasticity of the vestibulo-ocular reflex in monkeys. *J. Neurosci.* 6, 346–354.
- Mazurek, M., Kager, M., and Van Hooser, S.D. (2014). Robust quantification of orientation selectivity and direction selectivity. *Front. Neural Circuits* 8, 1–17.
- Mittmann, W., and Häusser, M. (2007). Linking synaptic plasticity and spike output at excitatory and inhibitory synapses onto cerebellar Purkinje cells. *J. Neurosci.* 27, 5559–5570.
- Rasmussen, A., Jireheden, D.-A., Zucca, R., Johansson, F., Svensson, P., and Hesslow, G. (2013). Number of spikes in climbing fibers determines the direction of cerebellar learning. *J. Neurosci.* 33, 13436–13440.
- Robinson, D.A. (1963). A method of measuring eye movement using a scleral search coil in a magnetic field. *Bio-Medical Electron. IEEE Trans.* 10, 137–145.
- Sarkisov, D. V., and Wang, S.S.-H. (2008). Order-dependent coincidence detection in cerebellar Purkinje neurons at the inositol trisphosphate receptor. *J. Neurosci.* 28, 133–142.
- Schindelin, J., Arganda-Carreras, I., Frise, E., Kaynig, V., Longair, M., Pietzsch, T., Preibisch, S., Rueden, C., Saalfeld, S., Schmid, B., et al. (2012). Fiji: an open-source platform for biological-image analysis. *Nat. Methods* 9, 676–682.